Canadian Geotechnical Journal

OPEN ACCESS | Research Article

Influence of depolymerized polyethylene terephthalate (PET) polymer on shrinkage and water retention characteristics of biochar-treated soil

Usmita Adhikari[a], **Sumi Siddiqua**[b], **and Alok Chandra**[a]

[a]School of Engineering, The University of British Columbia, Kelowna, BC V1V 1V7, Canada; [b]Faculty of Applied Science, The University of British Columbia, Kelowna, BC V1V 1V7, Canada

Corresponding author: **Sumi Siddiqua** (email: sumi.siddiqua@ubc.ca)

Abstract

The adoption of sustainable materials, such as biochar and polymers, for soil amendment provides a low-carbon alternative to establishing hydraulic barriers in waste disposal facilities. However, the unsaturated behaviour of the amended liner remains unexplored. The soil water characteristic curve (SWCC) and the soil shrinkage characteristic curve (SSCC) are key to understanding seepage and unsaturated soil resilience, as they provide intrinsic hydraulic and mechanical information required to model and predict the behaviour of unsaturated soils. Therefore, this study provides comprehensive experimental research on the development of SWCC and SSCC for liner soil amended with different dosages of biochar (0%, 5%, 15%, and 25%) and bis(2-hydroxyethyl) terephthalate (BHET) polymer (0%, 2%, and 3%). Various tests, like compressive strength, volumetric shrinkage, water retention, electrical conductivity, and scanning electron microscopy (SEM), were conducted. Results showed that compressive strength, water retention capacity, and electrical conductivity of the samples increased with biochar and polymer content, while higher biochar dosage decreased volumetric shrinkage significantly, indicating improved performance of liner soil. Moreover, SEM analysis showed the formation of polymer connections and films at the interparticle contacts of biochar and soil. The results are promising and provide a framework for using biochar and the BHET polymer as landfill liner materials.

Key words: biochar, bis(2-hydroxyethyl) terephthalate, soil water characteristics curve, soil shrinkage characteristic curve, suction, electrical conductivity

Résumé

L'adoption de matériaux durables, tels que le biochar et les polymères, pour l'amendement des sols constitue une alternative à faible empreinte carbone à l'établissement de barrières hydrauliques dans les installations d'élimination des déchets. Toutefois, le comportement non saturé du sol de revêtement amendé demeure peu exploré. La courbe caractéristique de rétention d'eau du sol (SWCC) et la courbe caractéristique de retrait du sol (SSCC) sont essentielles à la compréhension des écoulements et de la résilience des sols non saturés, car elles fournissent les informations hydrauliques et mécaniques intrinsèques nécessaires pour modéliser et prédire le comportement des sols non saturés. Par conséquent, cette étude présente une recherche expérimentale approfondie sur le développement des courbes SWCC et SSCC pour un sol de revêtement amendé avec différentes teneurs en biochar (0 %, 5 %, 15 % et 25 %) et en polymère bis(2-hydroxyéthyl) téréphtalate (BHET) (0 %, 2 % et 3 %). Divers essais, tels que la résistance à la compression, le retrait volumétrique, la rétention d'eau, la conductivité électrique et la microscopie électronique à balayage (MEB), ont été réalisés. Les résultats ont montré que la résistance à la compression, la capacité de rétention d'eau et la conductivité électrique des échantillons augmentaient avec la teneur en biochar et en polymère, tandis qu'une teneur plus élevée en biochar réduisait significativement le retrait volumétrique, indiquant une amélioration des performances du sol de revêtement. De plus, l'analyse par MEB a révélé la formation de liaisons et de films polymériques aux contacts interparticulaires entre le biochar et le sol. Les résultats sont prometteurs et fournissent un cadre pour l'utilisation du biochar et du polymère BHET comme matériaux de revêtement pour sites d'enfouissement.

Mots-clés : biochar, bis(2-hydroxyéthyl) téréphtalate, courbe caractéristique de rétention d'eau du sol, courbe caractéristique de retrait du sol, succion, conductivité électrique

1. Introduction

Landfills remain the predominant method for the secure disposal of municipal and hazardous wastes worldwide. Although modern landfills are generally engineered to high standards, the basal lining systems may still fail to fully prevent leachate migration and the infiltration of harmful substances into groundwater. Such failures can lead to the release of hazardous contaminants into adjacent water bodies and coastal environments (Rowe 2011; Alves de Godoy Leme and Gonçalves Miguel 2018; Mei et al. 2020). Contaminant transport through compacted liners is commonly evaluated assuming saturated flow during the design stage; however, in reality, landfill liners typically remain unsaturated. As a result, unsaturated water movement becomes a critical factor in predicting contaminant migration through these barriers and in safeguarding groundwater resources (Liu and Hu 2014; Khan et al. 2022). The soil water characteristic curve (SWCC) captures the relationship between soil suction and water content, reflecting the ability of soil to store or release water under different suction levels, and serves as a key tool for interpreting and estimating unsaturated soil property functions (Gitirana and Fredlund 2004). Likewise, the soil shrinkage characteristic curve (SSCC) depicts soil volume change with varying moisture content. Because soil shrinkage modifies the void ratio and thereby affects the SWCC, both SWCC and SSCC are important for evaluating desiccation, shrinkage, crack formation, and the long-term hydraulic performance of compacted barriers (Wen et al. 2021).

Clayey soils with clay contents in the range of 20%–30% are recommended for use as compacted clay liners (CCLs) in landfills (Daniel and Koerner 1993). However, compacted clays used as liners are prone to substantial shrinkage and desiccation cracking, which increase their hydraulic conductivity over time and undermine their effectiveness as barriers to leachate migration (Li et al. 2016). Desiccation cracking also reduces the strength of liner soils, leading to higher compressibility and excessive deformation (Albrecht and Benson 2001). To alleviate desiccation-induced shrinkage, various strategies have focused on modifying soil fabric using chemical additives. Biochar has recently gained attention as a promising landfill material due to its filtration capability, low volumetric shrinkage, and high water retention capacity (Reddy et al. 2015; Cai et al. 2022). Produced via thermochemical conversion of waste biomass under limited or no oxygen conditions, biochar offers the added benefit of supporting circular economy objectives by utilizing waste streams and enabling the production of efficient thermal backfill materials. Garg et al. (2019) demonstrated that biochar treatment can reduce gas permeability and shrinkage while improving water retention. Biochar can also increase the air entry value (AEV) and lower the soil desorption rate, thereby enhancing soil capillarity (Cai et al. 2022). Furthermore, biochar incorporation may alter the physicochemical properties of soil minerals, such as surface area, pore structure, and ion exchange capacity, through mechanisms involving surface complexation with hydroxyl groups or ion exchange with interlayer cations or anions (Wang et al. 2022). Experimental studies further indicate that the influence of biochar on soil behaviour is highly dependent on the dosage. At low to moderate contents (5%–10%), reductions in compressibility and improvements in shear strength have been reported (Reddy et al. 2015). Increasing biochar content has been shown to raise hydraulic conductivity and enhance soil water retention (Sun et al. 2020; Cai et al. 2022; Wan et al. 2022). An increase in electrical conductivity (EC) has also been observed in biochar-amended soils compared to untreated soils, attributed to ion release (Patwa et al. 2021). Despite improvements in water retention, a significant reduction in unconfined compressive strength (UCS) has been reported in biochar-treated soils (Patwa et al. 2024). The UCS is a critical parameter for landfill liners because it dictates the ability of the liner to maintain structural integrity and resist deformation under overburden and operational loads (Ni et al. 2020; Ramachandran et al. 2021). As a result, the application of biochar in field-scale liner systems remains somewhat constrained by this limitation.

A wide range of techniques for enhancing soil strength and lowering hydraulic conductivity have been reported in the literature. Chemical stabilizers, such as cement and lime, are commonly employed to improve soil durability and are generally regarded as cost-effective solutions. Little and Nair (2009) recommended combining clays with cement to enhance hydration and increase the strength of clay-soil mixtures. However, concerns regarding the environmental consequences of these materials have become more prominent in recent decades due to their substantial carbon emissions during production. Notably, cement manufacturing contributes approximately 8%–10% of global annual anthropogenic CO_2 emissions (Zhang et al. 2018; Andrew 2019). Consequently, there is growing interest in eco-friendly binders capable of improving both the strength and water retention characteristics of biochar-amended soils. Microbial-induced calcite precipitation (MICP)/enzyme-induced calcite precipitation (EICP) have gained recognition as a sustainable soil improvement technique due to its lower carbon footprint and its capacity to enhance mechanical performance (Li et al. 2023, 2024; Bhurtel et al. 2024). Recent advances have deepened the understanding of MICP/EICP-treated soils in relation to strength development, durability, and large-scale field performance under challenging environmental conditions (Chandra and Ravi 2020, 2021; Su et al. 2024; Dong et al. 2025). For example, water-glass-enhanced biocementation has been shown to accelerate early-age strength and improve cementation efficiency in sandy soils, providing valuable insight into MICP stabilization mechanisms (Dong et al. 2025). In addition, Su et al. (2024) proposed applying the MICP process for pore densification and surface modification of biochar to strengthen soil–biochar interactions. Parallel research efforts have examined polymers as environmentally compatible additives for soil stabilization. Motivated by these developments, the present study focuses on polymers as green binders to improve the engineering properties of biochar-amended soils. When polymers are used for soil modification, only small dosages (0.1%–5%) by weight are typically required to achieve strength improvements comparable to much larger cement dosages (3%–20%) by weight (Piqué et al. 2019; Chang et al. 2020; Chandra and Siddiqua 2022). Recent investigations have highlighted the effectiveness of polymer–clay combinations for strength improvement and hydraulic conductiv-

ity reduction in liners and cover systems. Gopakumar and Bharat (2025) employed xanthan gum (XG), a biopolymer, for slope stabilization in clayey soils, demonstrating its potential for applications such as landfill covers and liners, and canal lining to reduce infiltration and enhance stability. Despite its environmental compatibility, XG is susceptible to degradation under harsh field conditions (Moghal and Vydehi 2021).

Polyethylene terephthalate (PET), a common non-biodegradable polymer, constitutes a significant fraction of solid waste streams. Recent studies from our research group have examined the use of chemically depolymerized PET in the form of bis(2-hydroxyethyl) terephthalate (BHET) polymer (Chandra and Siddiqua 2022, 2023). BHET is produced by chemically depolymerizing PET waste through glycolysis with ethylene glycol under catalytic conditions, yielding BHET monomers after cooling and purification (Hernández et al. 2015; Şimşek 2020). BHET shares a similar molecular structure with PET and contains strong carbon–carbon (C–C) bonds, rendering it highly resistant to early-stage natural degradation. BHET is produced as white crystalline solids, and no harmful emissions or contamination associated with it have been reported (Taniguchi et al. 2019; Qiu et al. 2020). The hydroxyl (OH) and carbonyl (C = O) functional groups in BHET facilitate interactions with charged materials, including clays, semiconductors, and other polymers, promoting the formation of cross-linked structures (Liu et al. 2020; Chandra and Siddiqua 2022). For instance, Hernández et al. (2015) showed that the lone-pair electrons on the oxygen atoms within these groups enable coordination bonding with various toxic heavy metals. The properties of BHET have been assessed across a diverse range of civil engineering applications. Noteworthy examples include its use in concrete to enhance crack-healing behaviour, thermal and electrical responses, and durability (Şimşek 2020), as well as its function as a heavy-metal adsorbent for industrial wastewater treatment (Fatima et al. 2020). Furthermore, BHET has been incorporated into polymer–clay nanocomposites to improve thermal stability and gas barrier performance (Zhang et al. 2004; Chen et al. 2009). Chandra and Siddiqua (2022) evaluated BHET polymer content in sand–bentonite mixtures (SBMs) compacted at molding densities of 1.55, 1.65, and 1.75 g/cm^3 using three key criteria: low hydraulic conductivity (<10^{-7} cm/s), low volumetric shrinkage (<4%), and high UCS (>200 kPa). All three requirements, essential for landfill liner performance, were satisfied with a BHET content of 3% across the tested densities. One-dimensional consolidation testing by Chandra and Siddiqua (2023) further showed that the swollen BHET hydrogel induced pore-clogging, reducing both compressibility and hydraulic conductivity of the SBM as BHET content increased. Additionally, increasing the BHET content from 0% to 4% enhanced Pb^{2+} removal at all initial concentrations due to the additional adsorption sites provided by BHET functional groups.

Drawing from the above evidence, we hypothesize that the incorporation of BHET polymer into biochar-amended soils will result in a strong, durable, and environmentally sustainable composite suitable for landfill liner construction, with enhanced water retention and reduced volumetric shrinkage. Despite this potential, the interactions among BHET polymer, biochar, and soil remain uninvestigated in the existing literature. Moreover, to the best of the authors' knowledge, the effects on the SSCC and soil water retention curve (SWRC) in biochar-amended soils have not yet been explored. Only a limited number of studies have explored the use of BHET for soil stabilization. For instance, Al-Taie et al. (2020) evaluated the application of BHET polymer to reduce compressibility and increase direct shear strength in poorly graded sand, while Chandra and Siddiqua (2022, 2023) investigated BHET-treated SBMs to assess hydraulic conductivity and UCS for potential landfill cover and liner use. Thus, qualitative investigations are necessary to fully understand the influence of the polymer on biochar-amended soil and the resulting implications for the SSCC and SWRC before recommending the BHET–biochar–soil composite as a landfill liner material. Additionally, the impact of biochar and polymer amendments on the EC of compacted liners warrants further study. The relationship between EC and moisture content can provide valuable insights into moisture distribution, void formation, and structural heterogeneity within the liner (Kalinski and Kelly 1993; Pozdnyakov et al. 2006). Understanding how BHET addition influences the mechanical strength, moisture retention, and structural characteristics of biochar-amended soils is therefore essential. Evaluating the response of such soils to suction and stress will help identify the most suitable material combinations for liners and improve overall durability and performance.

In this investigation, the SWCC and SSCC of the BHET–biochar–bentonite–soil system are established to characterize seepage behaviour, unsaturated soil resilience, and associated hydromechanical properties. The research primarily examines the unsaturated behaviour of soils amended with biochar and BHET polymer, focusing on shrinkage, EC, and water retention performance of the composite liner material. A series of compressive strength, volumetric shrinkage, water retention, and EC tests was conducted, and scanning electron microscopy (SEM) was employed to assess microstructural features. This study underscores the potential for repurposing PET waste in hydraulic barrier construction due to its non-toxic nature, cementitious behaviour, heavy metal adsorption capacity, ready availability, and low biodegradability.

2. Materials and methods

2.1. Experimental materials

2.1.1. Soil

The soil used in this study was collected from a site adjacent to the Thompson River in Kamloops, British Columbia, Canada. Based on ASTM D-2487, the soil is classified as a well-graded, non-plastic silty sand (SM) (ASTM 2011). In many engineering projects, in-situ soils do not meet the required geotechnical standards for CCLs. Blending locally available silty sands with bentonite can provide the low hydraulic performance and adequate strength needed for liner systems

Fig. 1. Particle size distribution for the soils and biochar.

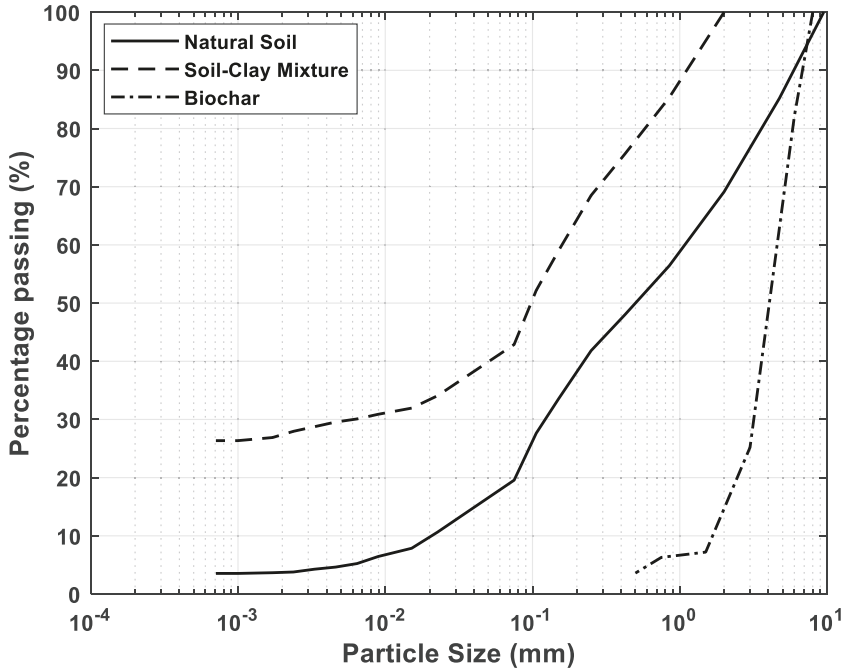

Table 1. Properties of biochar

Properties	Values
Density at 20 °C (kg/m^3)	150
Particle size (mm)	<2
Auto ignition temperature (°C)	450
pH	8.25
Water-holding capacity (%)	257.76
Specific surface area (m^2/kg)	371
Electrical conductivity (EC20 w/w) (mS/cm)	0.263
Ash content (%)	2.4
Volatile matter (%)	21.4
Organic carbon (%)	90.4
Hydrogen/carbon (H:C)	0.34
Nitrogen	0.59

while minimizing the transport of natural clays (Lima et al. 2026). For CCL construction, Daniel and Koerner (1993) recommended using soils containing approximately 20%–30% clay. In this research, soil passing the 2 mm sieve was used to prepare the soil–clay mixture (SCM). The bentonite employed was a sodium bentonite obtained from a local supplier in British Columbia, Canada. The particle-size distributions of both soils are shown in Fig. 1.

2.1.2. Biochar

The biochar is obtained from BC Biocarbon, which is manufactured at high temperatures between 600 and 800 °C, ensuring minimal bio-oil residues. The properties and particle size distribution curve of the biochar are given in Table 1 and Fig. 1, respectively. The biochar was finely ground using a grinder, and the powder that passed through a 2 mm sieve was used in this study.

2.1.3. Polymer

The BHET polymer used in this study was supplied by Sigma–Aldrich (Canada) as a powder. The BHET was ground and sieved through a 0.075 mm sieve before being mixed with the soil, bentonite, and biochar. The specific gravity of BHET is 1.316 g/cm^3, with a molecular formula $C_{12}H_{14}O_6$ and a molecular weight of 254.24 g/mol. Additionally, it features low viscosity and has a water solubility of 17.61 g/L (Chandra and Siddiqua 2023). Figure 2*a* presents the molecular structure of BHET, which consists of a benzene ring, two aromatic ester groups, two hydroxyl groups, and two primary alcohol functional groups (Chandra and Siddiqua 2022). Similarly, Fig. 2*b* illustrates the SEM image of the BHET polymer. Figure 2*c* illustrates the results of the BHET polymer for the Fourier transform infrared spectrometer test. It is acquired using the attenuated total reflectance (ATR) method in the wavelength range of 500–4000 cm^{-1}. The absorption band at 726 cm^{-1}, signal at 1277 cm^{-1}, peak at 3444 cm^{-1}, and adjacent peaks at 2880 and 2964 cm^{-1} represent the presence of a benzene ring, C–O–C stretching vibrations in ester groups, O–H stretching of hydroxyl groups and alcoholic groups, respectively (Castaño et al. 1998; Zhou et al. 2012; Chandra and Siddiqua 2022).

2.2. Experimental methods

2.2.1. Specimen preparation

This study investigates the influence of biochar and BHET polymer on the SWCC and SSCC of the soil. Specimens were

Fig. 2. (*a*) Molecular structure of bis(2-hydroxyethyl) terephthalate (BHET) polymer, (*b*) scanning electron microscopy image of BHET powder, and (*c*) Fourier transform infrared spectra for BHET polymer.

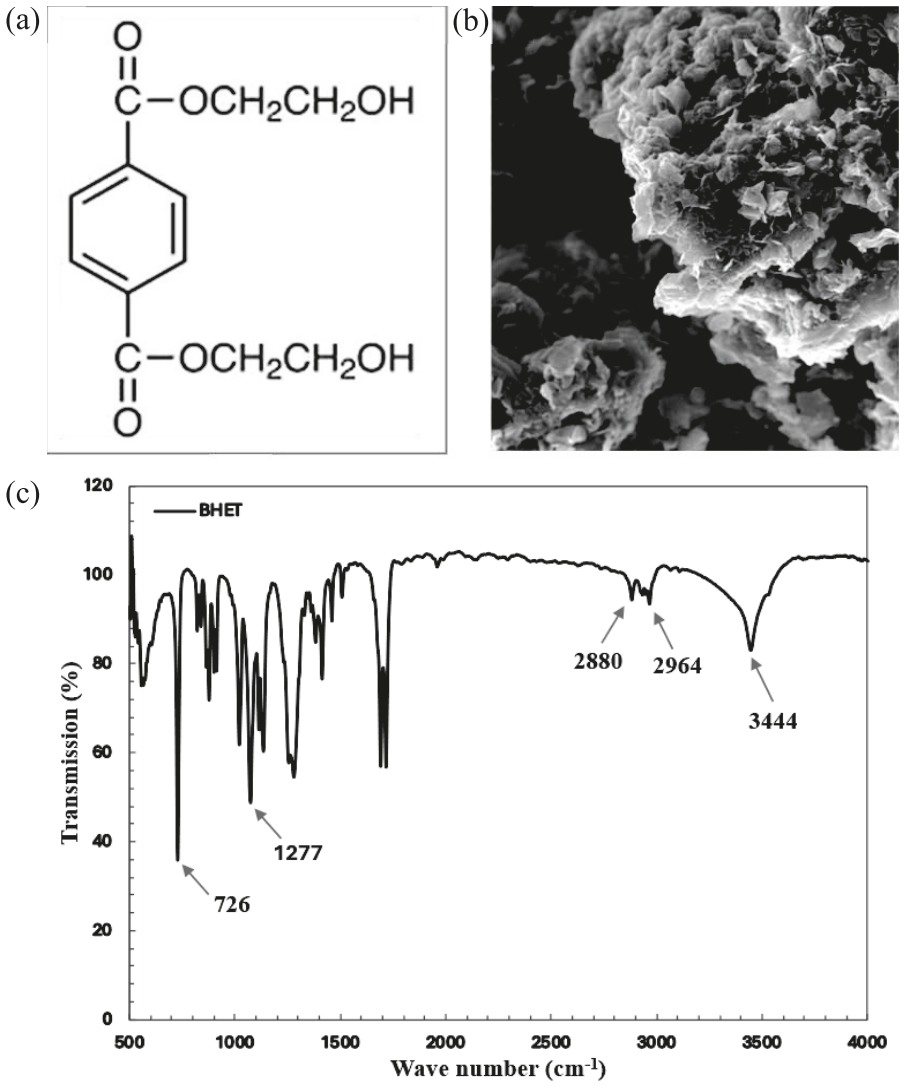

prepared with four biochar dosages (0%, 5%, 15%, and 25% by dry weight of the SCM), and for each biochar level, three BHET polymer dosages (0%, 2%, and 3% of SCM) were produced. Prior to mixing, the soil, bentonite, and biochar were oven-dried and cooled, then blended with BHET to form a dry mixture; deionized water was subsequently added to prepare the specimens. The maximum dry density (MDD) and optimum moisture content (OMC) for each composition were determined using the Standard Proctor test in accordance with ASTM D698 (2012). The Atterberg limits, including liquid limit (LL%) and plastic limit (PL%), were measured following ASTM D4318 (2017), and pH was evaluated according to ASTM D4972 (2019). For SWCC, SSCC, EC, and SEM analyses, specimens were compacted at their respective OMC and MDD to ensure consistent initial conditions. Before compaction, the wetted mixtures were sealed in plastic bags and stored at room temperature for 24 h to achieve equilibrium moisture content. All tests were conducted in triplicate within a humidity- and temperature-controlled chamber, resulting in a total of 36 soil specimens. The OMC, MDD, LL, PL, and pH values for all mixtures are summarized in Table 2.

2.2.2. Soil water characteristic curve

The relative humidity (RH) sensor (Rotronics Hygroclip Relative Humidity Sensor–model # HC2-S) was used to measure the RH at different moisture contents for each specimen. The RH sensors were calibrated using six calibration points, including five different oversaturated binary salt solutions and deionized water. The RH sensor was first connected to a suction tip, as shown in Fig. 3, and then inserted into a hole drilled at the bottom of previously saturated specimens (Tabiatnejad et al. 2016). A broad range of moisture content was established to get a full SWCC. After each RH measurement, the specimen was left to dry until it reached the desired water content for another RH reading, which was confirmed by regular mass measurements. After taking all the desired readings, the samples were dried in an oven to deter-

Table 2. Physical characteristics of the samples.

Specimen	B (%)	P (%)	OMC (%)	MDD (g/cm^3)	LL (%)	PL (%)	pH
SCM-0B-0P	0	0	17.50	1.83	79.00	24.75	6.10
SCM-5B-0P	5		17.50	1.68	79.00	24.72	7.92
SCM-15B-0P	15		25.80	1.33	83.26	22.65	8.48
SCM-25B-0P	25		33.50	1.13	87.60	20.89	8.95
SCM-0B-2P	0	2	18.90	1.80	87.52	30.19	5.52
SCM-5B-2P	5		19.00	1.70	87.58	30.22	7.16
SCM-15B-2P	15		27.20	1.36	91.00	28.31	7.45
SCM-25B-2P	25		34.90	1.15	96.21	27.42	7.62
SCM-0B-3P	0	3	19.80	1.78	89.42	35.25	4.53
SCM-5B-3P	5		20.10	1.71	89.48	35.38	6.22
SCM-15B-3P	15		28.30	1.37	101.04	39.49	6.55
SCM-25B-3P	25		36.00	1.17	107.15	38.46	6.81

Note: B = biochar content; P = BHET polymer content

Fig. 3. Suction tip and relative humidity sensor to measure relative humidity.

mine the final water content. Once the RHs in soil specimens were measured, total suctions were calculated using Kelvin's equation (Fredlund and Rahardjo 1993).

$$(1) \qquad \psi = -\frac{RT}{M_w\left(\frac{1}{\rho_w}\right)} \cdot \ln(RH)$$

where ψ is total suction in soil (kPa), R is the universal (molar) gas constant (8.314 J/mol·K),

RH is the relative humidity (expressed as a fraction between 0 and 1), T is the absolute temperature (K), M_w is the molecular mass of water (18.016 kg/kmol), and ρ_w is the density of water (kg/m^3).

The gravimetric water content of each specimen was measured before and after the RH test. The sigmoidal equation derived by van Genuchten (1980) was used to best fit the SWCC data based on the gravimetric water content designation:

$$(2) \qquad S_r = \frac{\theta - \theta_r}{\theta_s - \theta_r} = \left[\frac{1}{1 + (\alpha\psi)^n}\right]^m$$

where θ is a given volumetric moisture percentage; θ_r and θ_s are residual and saturated volumetric water contents, respectively; α is the inverse of the AEV; and n and m are fitting parameters.

2.2.3. Volumetric shrinkage

For the shrinkage test, samples compacted at OMC and MDD, measuring 63 mm in diameter and 22 mm in height, were fully saturated. The saturated soil specimens were kept in a chamber with controlled humidity (60 ± 2%) and temperature (23 ± 2 °C). The diameter and height of each sample were measured at regular intervals along the drying path using a digital vernier caliper until no further volume change was observed. At the same interval of dimension measurement, the soil specimen was placed on a precision weighing scale to measure the corresponding gravimetric water content. The volumetric properties of the soil specimens were adjusted to account for the addition of biochar. The void ratio of the biochar-amended soil was calculated using the following equation (Cai et al. 2022):

$$(3) \qquad e = \frac{e_0 - R_B(1 + e_0)}{1 + R_B(1 + e_0)}$$

Fig. 4. Soil water characteristic curve for biochar-treated soil–clay mixture (SCM) at (*a*) 0% bis(2-hydroxyethyl) terephthalate (BHET), (*b*) 2% BHET, (*c*) 3% BHET, (*d*) effect of BHET polymer content on air entry value at varying biochar content.

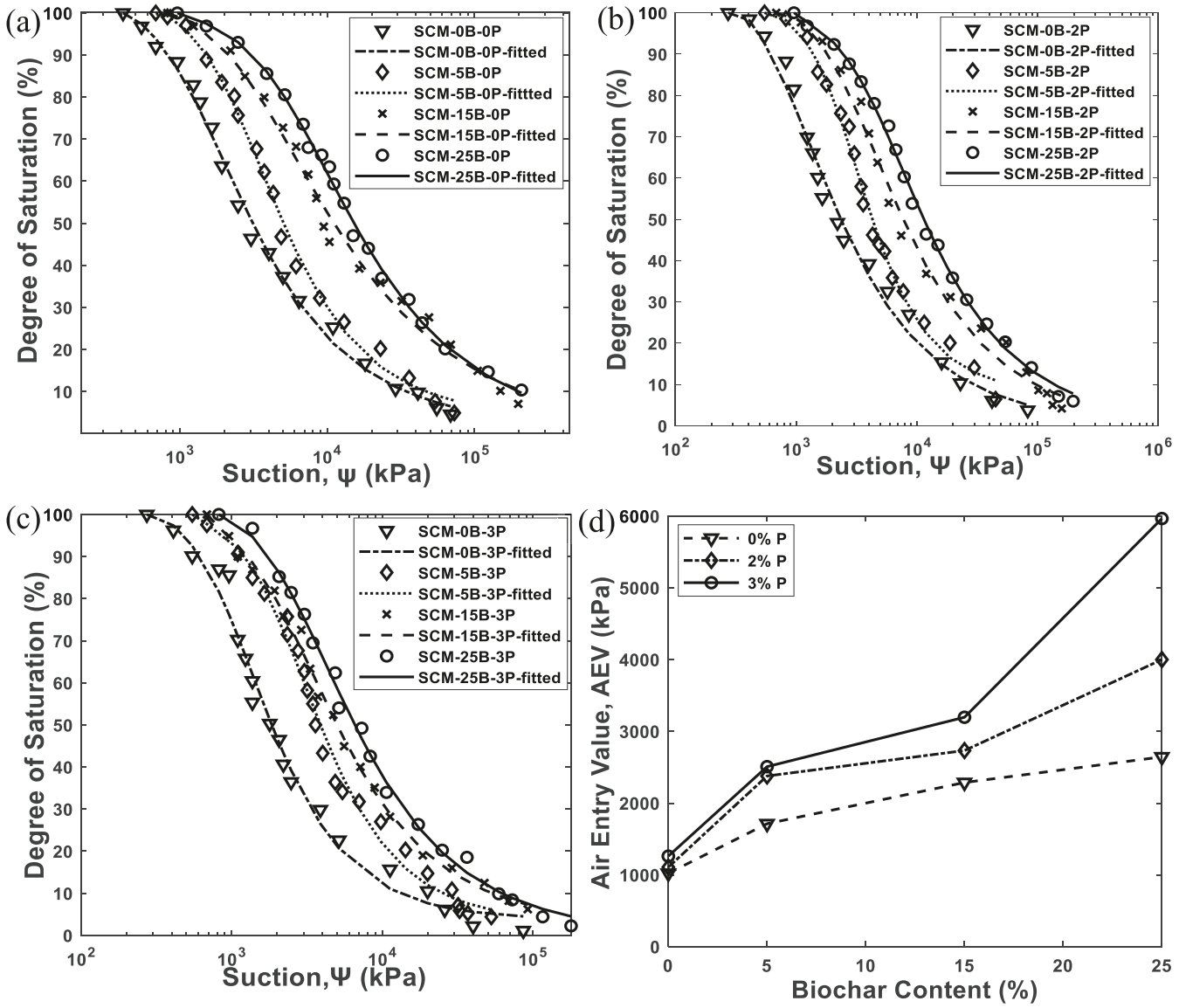

where e_0 represents the initial void ratio of the soil, and R_B is the ratio of the total volume of biochar per unit volume of soil.

Data points from the measured shrinkage curve were fitted using the model proposed by Fredlund et al. (2002) to derive the SSCC. In this model, volume change, expressed in terms of void ratio (e), for deformable soils is represented as a function of gravimetric water content (w).

$$e(w) = e_{\min}\left[\left(\frac{w}{S_L}\right)^{C_{sh}} + 1\right]^{1/C_{sh}} \quad \text{and,} \tag{4}$$

$$\frac{e_{\min}}{S_L} = \frac{G_s}{S_0} \tag{5}$$

where, $e_{\min}$ is the minimum void ratio attained during the shrinking process, S_L represents the shrinkage limit, C_{sh} is the curvature of the shrinkage curve, G_s is the specific gravity, and S_0 is the initial degree of saturation.

2.2.4. Electrical conductivity

The soil sample was compacted to a height of 50 mm with a diameter of 40 mm at its OMC and MDD. A hole was drilled at the bottom of saturated samples, like the RH test samples. An EC meter was then used, with its probe inserted into the drilled hole to record the EC at various moisture levels (Arnold et al. 2005). The electrical characteristic of soil is frequently represented by the soil resistivity value (ρ) or soil EC (σ) (Heaney 2003; Samouëlian et al. 2005)

$$\rho = \frac{1}{\sigma} \tag{6}$$

A wide range of water content was tested to observe the general trend of change in conductivity with moisture varia-

tion in soil samples mixed with biochar and BHET polymer. After each measurement, the samples were allowed to dry to the following target moisture content, with mass measurements taken to verify the water level before the subsequent readings. At the end of testing, the samples were oven-dried to determine the final moisture content.

2.2.5. Unconfined compressive strength

The UCS of the biochar and BHET polymer amended SCM composites was determined according to ASTM D2166 (ASTM D2166 2006). The UCS test was conducted to assess the strength properties of the composites and to investigate the influence of the additives on the clay. Specimens were prepared by compacting the mix at their OMC and MDD in three equal layers in a 38 mm diameter and 76 mm height mold. The samples were then taken out with a hydraulic jack after compaction, wrapped in layers of cling film, and left to cure for 1 day and 28 days in an environment with a RH of 60 ± 2% and a controlled temperature of 23 ± 2 °C. According to Smitha et al. (2021), Vydehi and Moghal (2022), and Chandra and Siddiqua (2023), a 28-day curing period is recommended for evaluating and comparing the long-term effects of polymer treatment on strength. A total of 36 soil specimens, containing three replicas of each composition, were prepared for all testing to ensure the consistency and reproducibility of the results. A constant vertical load rate of 0.8 mm/min was applied to the specimens until the sample failed.

2.2.6. Scanning electron microscopy

A small sample of soil was collected from both the untreated and treated soil mixture specimens. After oven drying, the samples were attached to aluminium pin stubs and coated with a 10 nm thick platinum layer to minimize surface charging and improve secondary electron emission. Following the coating, imaging was conducted using a Tescan Mira 3 XMU SEM.

3. Results and discussions

3.1. Effect of BHET on soil water characteristics curve

Figures 4*a*–4*c* illustrates the SWCCs of the biochar-amended SCM at various BHET polymer dosages, respectively. The van Genuchten (1980) closed-form equation is used to fit the collected data points, and the fitting coefficients for each soil specimen are presented in Table 3. The "*n*" value, an essential parameter of the fitting curve, has followed a decreasing trend with the biochar and the polymer treatment, except for samples with 5% biochar. A decreased "*n*" value flattens the SWCC, Fig. 4*a*–4*c*, indicating a wider pore-size distribution and soil holds more water at higher suctions and reduces moisture loss. This characteristic can decrease shrinkage and cracking under drying conditions (Wan et al. 2018, 2021). Polymers with the capacity to form hydrogels, i.e., BHET, bind water and coat soil particles, reducing drainage. Hence, the

Table 3. Summary of fitting coefficients for soil water characteristic curve.

	van Genuchten (1980) model			
Specimen	θ_s (m^3/m^3)	θ_r (m^3/m^3)	n	AEV ($1/\alpha$), (kPa)
SCM-0B-0P	39.78	1.43	2.09	1022.97
SCM-5B-0P	42.21	2.00	2.09	1713.56
SCM-15B-0P	49.16	1.13	1.81	2287.72
SCM-25B-0P	57.89	1.55	1.76	2644.94
SCM-0B-2P	43.14	0.61	1.66	1107.90
SCM-5B-2P	43.56	3.30	2.15	2378.54
SCM-15B-2P	51.95	1.13	1.66	2732.97
SCM-25B-2P	57.92	1.55	1.69	4000.53
SCM-0B-3P	41.99	0.61	1.76	1261.81
SCM-5B-3P	45.44	1.66	1.95	2508.72
SCM-15B-3P	52.33	1.13	1.56	3196.81
SCM-25B-3P	58.59	1.55	1.71	5965.71

Note: SCM, soil–clay mixture; AEV, air entry value.

"*n*" value is lowered with biochar and polymer content. Nevertheless, the water-holding capacity of the specimens improved with increasing biochar and BHET treatment rates. Samples with 25% biochar and 3% polymer exhibit superior water retention capacity. The significant pore size and elevated surface area of biochar are attributed to enhanced water retention capacity (Cai et al. 2022).

The comparison of AEV for different dosages of biochar- and polymer-treated SCM is shown in Fig. 4*d*. As shown in Fig. 4*d*, the AEV of the specimens increased significantly with the increase of BHET dosage in the biochar-treated soil. With the addition of 2% BHET polymer to 5% biochar-amended SCM, the AEV increased by 38.4%. However, small changes in AEVs were observed upon adding BHET to specimens without biochar. The most significant increase in AEV was observed for SCM-25B-3P, with a 582.3% improvement over the control specimen (SCM only). The significance of higher AEV in landfill liner design lies in the capacity of soil to remain saturated under varying suction environments, which directly influences the effectiveness of the liner as a hydraulic barrier. A similar trend of rising AEV values is also reported for soil amended with biochar (Wang et al. 2019; Cai et al. 2022). However, the values of *n*, one of the fitting parameters of SWCC, showed no notable trend with increases in the biochar and polymer percentages.

The enhancement of SWCC depends on soil factors, including texture, mineralogy, and cation exchange capacity. Biochar-treated soils show greater AEV improvement due to a change in particle orientation, a condition facilitated by the addition of biochar (Bhardwaj et al. 2009; Öncü and Bilsel 2017; Cai et al. 2022). Furthermore, adding BHET polymer improves surface soil moisture retention by forming a hydrogel network, enhancing water accessibility. The incorporation of BHET polymer generates a hydrogel that electrostatically bonds with soil/bentonite particles via ion-dipole interactions and/or hydrogen bonding, resulting in a polymer hydrogel–soil matrix that establishes a cohesive pore structure inside the biochar (Narjary et al. 2012; Saha et al. 2021). This results in the modification of soil pore geometry and

Fig. 5. A conceptual model for mechanisms for water retention: (*a*) biochar-soil–clay mixture (SCM) composite and (*b*) bis(2-hydroxyethyl) terephthalate–biochar-SCM composite.

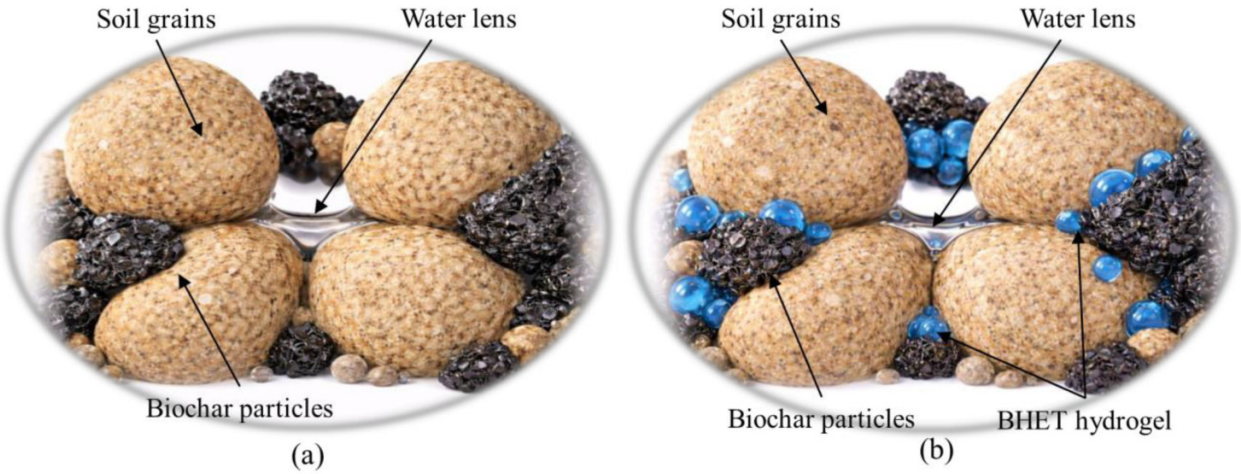

an associated elevation in the soil water characteristics curve due to the prevalence of a capillary pore water system (Ng and Pang 2000; Salager et al. 2013). A rise in the moisture retention capacity of soil with higher polymer content has been documented (Ni et al. 2020; Mahamaya et al. 2021).

The porous structure of biochar holds moisture, while the BHET polymer forms a network of hydrogel that swells upon hydration and locks moisture within its cross-linked matrix, as explained in the conceptual diagram in Fig. 5. Therefore, in the BHET–biochar–soil matrix, this mechanism enhances moisture retention beyond pore storage, thereby reducing moisture loss even at high suction conditions. A higher percentage of polymer in a denser configuration tends to hold moisture as a robust hydrogel, hence minimizing shrinkage. Pham et al. (2021) studied the behaviour of dry BHET at 33%, 55%, and 75% RH, observing weight gain due to moisture absorption. Şimşek (2020) found that BHET improved water absorption in concrete blocks due to its hydrophilic nature, leading to the formation of additional cement hydration products, including C–S–H gels and calcium hydroxide.

Jing et al. (2022) have documented the filling of clay particles within the intrapore structure of biochar. The clay adsorbed onto the exterior surface of biochar through "Ca^{2+} bridging," likely inducing a flexible deformation of the clay layers, which in turn facilitated the passage of the space between layers (Yang et al. 2021). Likewise, Jing et al. (2022) discovered a significant presence of hydrophilic functional groups in biochar produced from cellulose-rich biomass waste. This promotes the collaboration among biochar and soil minerals, resulting in the production of organo-mineral compounds (i.e., C–O–Al). It may boost water retention, as reflected in an increase in AEV (Fig. 4*d*), and expand the clay interlayer spacing. The porous structure of biochar facilitates moisture retention in SCM altered with biochar during desiccation-induced shrinkage. In the BHET polymer-treated, biochar-amended SCM, more water is needed to reach saturation compared to the biochar-amended SCM alone because the polymer increases water retention. Following pore saturation, any residual unreacted BHET may swell, generating hydrocolloids that subsequently reduce the pore diameters of the biochar–soil matrix (Chandra and Siddiqua 2022). Smaller pores can hold water more effectively due to capillary forces, and the water requires higher suction for extraction (Yin and Vanapalli 2022). Thus, the findings of the present study suggest that biochar-amended soil, incorporating BHET polymer, can serve as an effective adsorption medium while enhancing the shrinkage potential of the composite material. Furthermore, the drying SWRC shows substantial changes in both the AEV and the desorption rate with the incorporation of biochar into the soil at varying BHET concentrations.

3.2. Effects of BHET on soil shrinkage characteristic curve

Figures 6*a*–6*c* demonstrates the relationship between gravimetric water content and the void ratio of biochar-amended SCM at varying BHET polymer content. SSCC is regarded as a crucial constitutive relationship for interpreting the mechanical and hydraulic behaviour of unsaturated soils. The Fredlund et al. (2002) model was used to fit the collected data points, and the results are outlined in Table 3. The model parameters exhibit significant volumetric characteristics, such as shrinkage limit and void ratio of SCM with different biochar and BHET polymer content, as they dehydrate. The shrinkage curves for all investigated specimens exhibited three distinct phases: capillary shrinkage phase, pendular shrinkage phase and no shrinkage phase (Chen and Lu 2018). During the capillary phase, a reduction in pore water volume in a saturated state will correspondingly reduce bulk soil volume. Consequently, the shrinkage curve initially follows a diagonal line, as seen in Figs. 6*a*–6*c*, where its gradient is equal to 1 (Chertkov 2000). As drying progresses, air infiltrates the intra-aggregate pores, and the rate of water loss exceeds the reduction in void or bulk soil volume, marking the beginning of the pendular shrinkage phase. Further drying causes the SSCC to gradually level off after reaching the shrinkage limit (S_L), indicating that the bulk soil has attained

Fig. 6. Soil shrinkage characteristic curve of biochar-treated soil–clay mixture (SCM) at (*a*) 0% bis(2-hydroxyethyl) terephthalate (BHET), (*b*) 2% BHET, (*c*) 3% BHET, and volumetric shrinkage versus biochar-treated SCM at (*d*) 0% BHET, (*e*) 2% BHET, (*f*) 3% BHET.

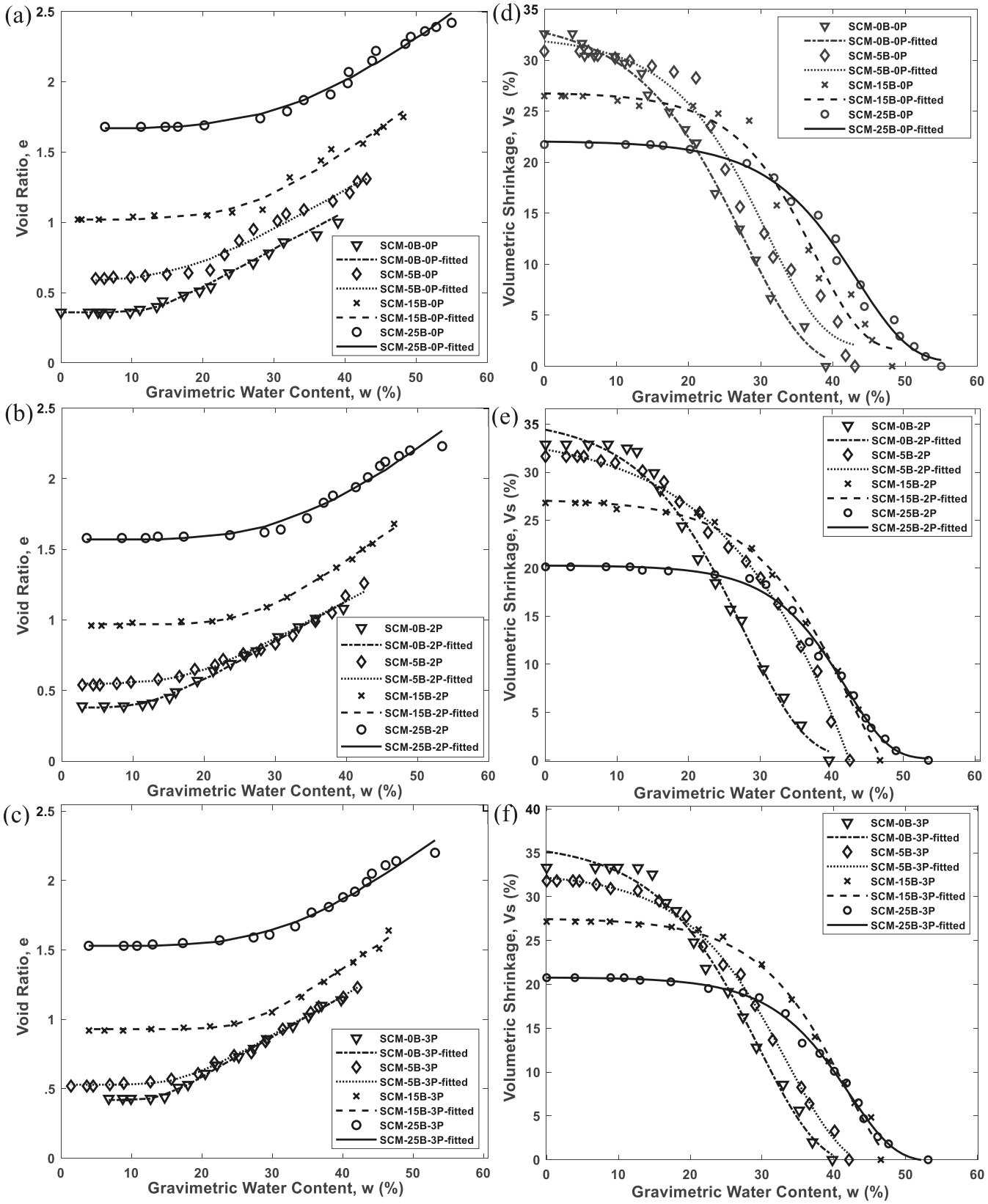

its densest state, as illustrated in Figs. 6*a*–6*c*. No shrinkage characterizes this stage, as the overall soil volume remains unchanged despite a further reduction in water content. The void ratio associated with this soil volume is at its minimum, also known as a minimum void ratio (e_{min}). The e_{min} estimated using the Fredlund et al. (2002) model for all specimens is

Fig. 7. Effects of the bis(2-hydroxyethyl) terephthalate polymer and the biochar content on (*a*) minimum void ratio and (*b*) shrinkage limit.

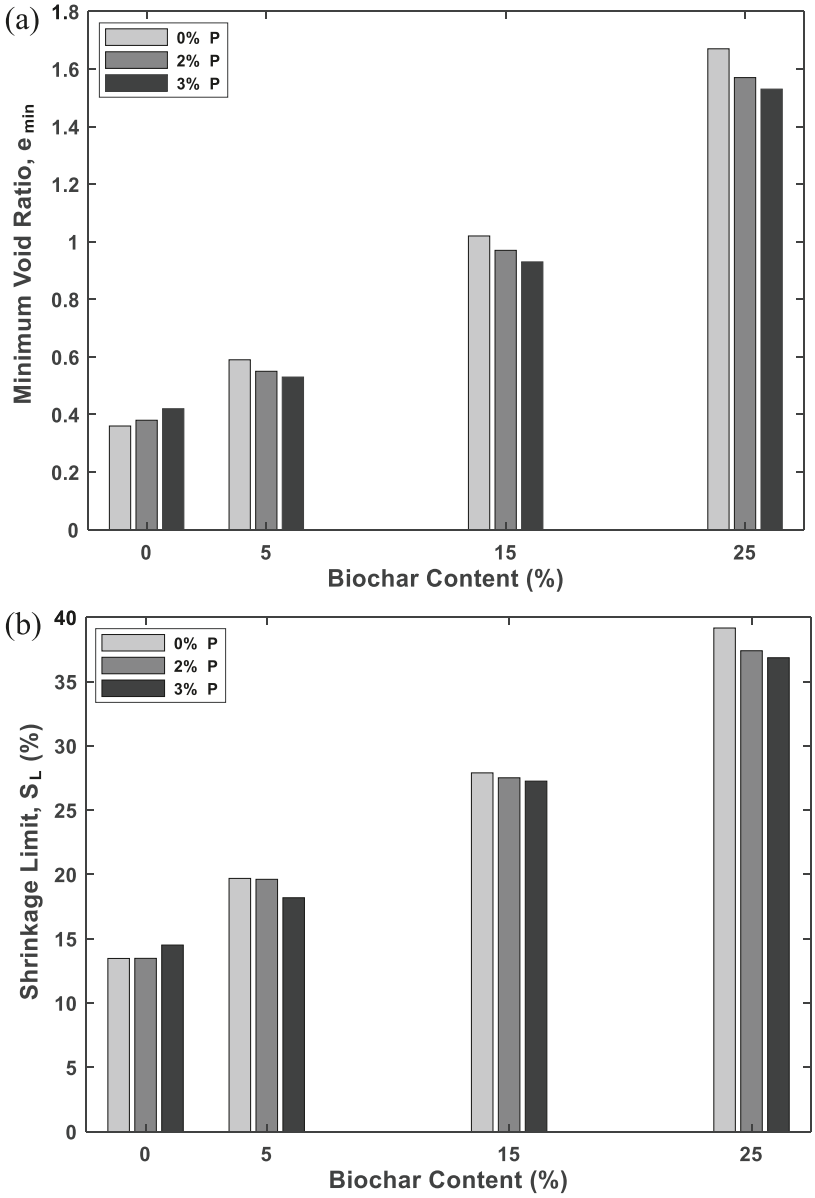

presented in Fig. 7*a*. Figure 7*a* demonstrates a fall in e_{min} for biochar-amended SCM with BHET polymer treatment, which indicates that an increase in polymer content mitigates the alteration in void ratio for soil. In Fig. 7*a*, the e_{min} increased by 62.5% for the specimen SCM-5B-0P compared to SCM-0B-0P, which demonstrates that e_{min} generally increases with a higher proportion of biochar.

Similarly, SSCC for SCM treated with varied BHET content is shown in Figs. 6*b* and 6*c*. Figures 6*b* and 6*c* for 2% BHET and 3% BHET indicate that the presence of the polymer results in a decrease of the initial void ratio that at 0% BHET, as reported in Fig. 6*a*, demonstrating a downward shift in the void ratio-gravimetric water content curves. The decrease in the void ratio is attributed to the substantial water-absorbing capacity of hydroxyl groups (−OH) in the BHET polymer, which retains water as a hydrogel, coating the voids created by biochar and resulting in a denser SCM structure. The combination of biochar and a polymer can alter the soil microstructure. Moreover, BHET acts as a binding agent, which results in a more compact structure by bringing soil particles and biochar closer together (Shen and Wei 2018; Şimşek 2020). An experimental study performed by Chandra and Siddiqua (2022, 2023) on BHET-treated SBM indicated that BHET treatment exhibited enhancement in geotechnical properties, such as increased shear strength and decreased compressibility. These enhancements also suggest that the combined amendments can alter the soil fabric, thereby decreasing void spaces.

The fitted S_L derived from the Fredlund et al. (2002) model for each of the studied specimens is plotted in Fig. 7*b*. Table 4

Table 4. Fitting parameters for soil shrinkage characteristic curve using Fredlund et al. (2002) model.

	Fredlund et al. (2002) model			
Specimen	e_{min}	S_L (%)	C_{sh}	R^2
SCM-0B-0P	0.36	13.46	7.27	0.98
SCM-5B-0P	0.59	19.69	3.52	0.85
SCM-15B-0P	1.02	27.89	5.52	0.85
SCM-25B-0P	1.67	39.16	9.00	0.98
SCM-0B-2P	0.38	13.47	4.65	0.98
SCM-5B-2P	0.55	19.61	4.63	0.96
SCM-15B-2P	0.97	27.51	7.45	0.97
SCM-25B-2P	1.57	37.39	4.48	0.97
SCM-0B-3P	0.42	14.50	10.24	0.99
SCM-5B-3P	0.53	18.18	4.96	0.99
SCM-15B-3P	0.93	27.25	10.35	0.99
SCM-25B-3P	1.53	36.85	4.51	0.98

Note: SCM, soil–clay mixture.

shows that the S_L parameter increases with increasing BHET concentration in soil. For instance, S_L rises by 7.75% as the BHET dosage increased from 0% to 3% in SCM. For biochar, SL increased by 46.25% in the SCM-5B-0P specimen compared to SCM-0B-0P. The incorporation of biochar into clay diminishes its volumetric shrinkage. The porous structure of biochar facilitates moisture retention, thereby reducing the potential for severe desiccation in SCM (Lu et al. 2014; Reddy et al. 2015). Zong et al. (2014) reported that the reduction in shrinkage is due to changes in the shrinkage behaviour of clay minerals resulting from the incorporation of biochar-derived carbon particles into the bentonite composite. The S_L increases with the addition of biochar to the SCM, indicating that the volumetric shrinkage of the soil during desiccation will be lower than that of unamended SCM samples. However, the inclusion of BHET led to a slight decrease in the S_L, as shown in Fig. 7*b*. This is attributed to flocculation of clay particles induced by the BHET polymer, resulting in decreased S_L compared to biochar alone.

Figures 6*d* –6*f* represent the relation between gravimetric water content and the volumetric shrinkage of SCM at varying biochar and BHET concentrations. Volumetric shrinkage decreases with increasing biochar and BHET content. When BHET polymer is combined with soil and water, it envelops the surfaces of soil grains and clay particles through electrostatic, ion-dipole, and hydrogen-bonding interactions. Furthermore, the BHET polymer interconnects to form a chain of viscous hydrocolloids that encapsulate soil and biochar clusters, thereby establishing a robust, finely porous framework. Upon saturation of the pores, any loose BHET that may have remained unreacted with water during mixing is likely to swell, forming hydrocolloids that subsequently reduce pore dimensions. By limiting the size of pores, the volume of the SCM samples stays more constant, decreasing the amount of shrinkage during drying (Chandra and Siddiqua 2022). Moreover, the higher moisture level at the higher polymer concentration prevents capillary force from developing and causing particle shrinkage. Shin et al. (2021) demonstrated that polymer-treated soil exhibited reduced shrinkage due to its superior moisture retention capacity. Similarly, in this study, the biochar and polymer treatment of SCM specimens resulted in enhanced water retention capacity, leading to a lower void ratio and reduced shrinkage. Numerous other studies, including sodium-bentonite with sodium carboxymethyl cellulose (Taheri and El-Zein 2025) and Polyvinyl acetate-treated expansive soil (Liu et al. 2017), have experimentally supported the reduction of the shrinkage potential of polymer-treated specimens compared to untreated ones.

3.3. Correlation between void ratio and suction

Figures 8*a*–8*c* illustrates the relationship between the suction and the void ratio of the specimens with varying dosages of biochar and BHET polymer. The correlation between void ratio and suction in the compacted liner is essential to understanding the unsaturated soil behaviour. This relationship helps regulate volumetric changes, moisture retention, and the overall mechanical properties of the soil. Figures 8*a*–8*c* exhibit an inverse correlation between void ratio and suction, with a high coefficient of determination ($R^2 > 0.95$), demonstrating a strong statistical fit. This relationship is represented by eq. 7, with corresponding fitting parameters listed in Table 5.

$$e = d + \frac{e_{min} - d}{1 + \left(\frac{\Psi}{(AEV)}\right)^b} \quad (7)$$

where e = void ratio, e_{min} = minimum void ratio, Ψ = suction (kPa), AEV = air entry value, and a, b, and d are fitting parameters, respectively.

In Figs. 8*a*–8*c*, the void ratio of the specimens increases with the increase in suction. Research demonstrates that an increase in suction typically results in a reduction in the void ratio due to shrinkage and densification of the soil matrix. Prior studies (Alonso et al. 1990; Fredlund and Rahardjo 1993) indicate that increased suction enhances effective stress, leading to soil densification and a reduction in void ratio. The BHET polymer functions as a binding agent, facilitating interaction between soil and biochar and potentially reducing the spacing between soil particles by promoting closer packing. The hydrophilic groups of hydroxyls (−OH) in BHET polymer have the capacity to absorb and hold substantial quantities of water molecules (Chandra and Siddiqua 2022, 2023). Consequently, the moisture content increases with polymer dosage, even at higher suction levels, inhibiting the development of capillary forces and preventing particle contraction. This results in a reduced void ratio and increased suction (Chang et al. 2020; Chandra and Siddiqua 2022; Wan et al. 2022).

3.4. Electrical conductivity

This study examined the EC of compacted samples as a function of degree of saturation, as depicted in Figs. 9*a*–9*c*. Figure 9*d* illustrates the EC of the samples at OMC. The measured results demonstrate that the EC of all the samples increases, following a sigmoidal trend with an increase in the degree of saturation. A similar trend of EC (inverse of resistivity) with water content has also been reported by Pozdnyakov

Fig. 8. Correlations between void ratio with suction of soil–clay mixture (SCM) at (*a*) 0% bis(2-hydroxyethyl) terephthalate (BHET), (*b*) 2% BHET, and (*c*) 3% BHET.

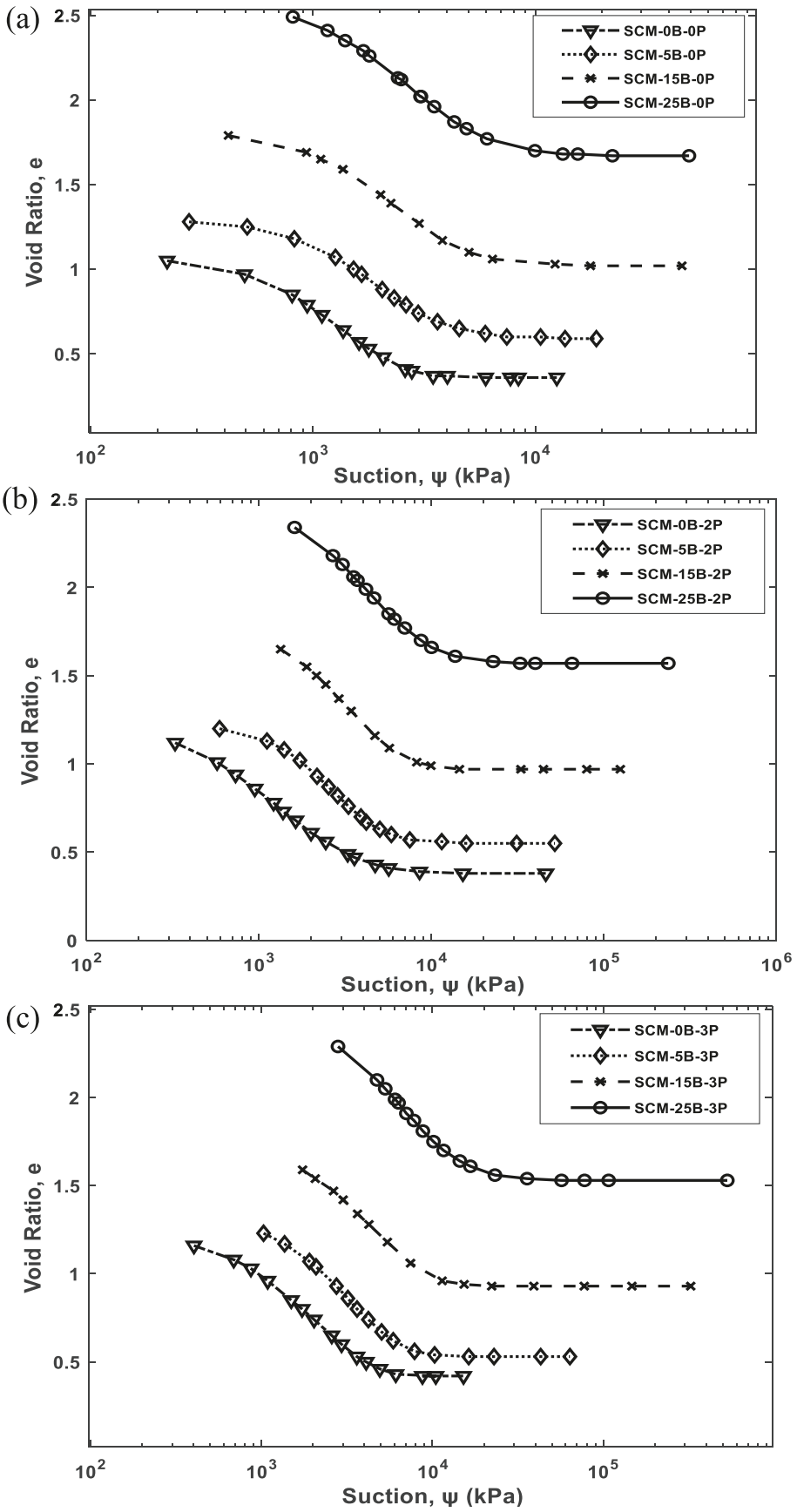

Table 5. Fitting parameters for void ratio and suction correlation.

Specimen	Fitting parameters				
	a	b	AEV (kPa)	d	R^2
SCM-0B-0P	0.35	− 2.61	1022.97	1.05	0.99
SCM-5B-0P	0.58	− 2.38	1713.56	1.28	0.99
SCM-15B-0P	1.01	− 2.29	2287.72	1.80	0.99
SCM-25B-0P	1.66	− 2.17	2644.94	2.55	0.99
SCM-0B-2P	0.37	− 1.74	1107.90	1.19	0.99
SCM-5B-2P	0.54	− 2.64	2378.54	1.21	0.99
SCM-15B-2P	0.96	− 2.61	2732.97	1.72	0.99
SCM-25B-2P	1.56	− 2.20	4000.53	2.44	0.99
SCM-0B-3P	0.39	− 2.09	1261.81	1.18	0.99
SCM-5B-3P	0.53	− 2.58	2508.72	1.27	0.99
SCM-15B-3P	0.93	− 2.51	3196.81	1.65	0.99
SCM-25B-3P	1.53	− 2.30	5965.71	2.40	0.99

Note: SCM, soil–clay mixture; AEV, air entry value.

et al. (2006) and Kibria and Hossain (2012, 2015). Prior research also demonstrates that biochar and polymers significantly influence soil EC. Conductivity is influenced by pore structure and increases with increased microstructural densification of materials (Bai et al. 2010; Kibria and Hossain 2012; Şimşek 2020). The charge mobility is enhanced as adsorbed charges are released into the solution with increasing soil water content. Furthermore, an increase in soil saturation correlates with enhanced particle bridging. The interconnection within the pore network is enhanced due to the diminishment of dielectric air voids at increased saturation levels (Kibria and Hossain 2012). Consequently, moisture bridging and the mobility of electrical charges facilitate the conduction of electrical current within a soil mass, leading to increased conductivity with moisture levels. This response strongly indicates that water serves as the medium for current flow in the compacted specimens, as shown in Figs. 9*a*–9*c*. At an equivalent saturation level, the EC of samples saturated with polymer is slightly higher than that of samples without polymer, indicating that polyvalent cation bridging elevates EC. A similar trend is observed with biochar, which improves soil water retention and facilitates greater ion mobility within soil pores due to its high porosity, surface functional groups, and enhanced liquid-phase connectivity that collectively support the dissolution and transport of ions. The highest EC is observed in the samples with 3% BHET and 25% biochar, with a value of 3.95 mS/cm at OMC. This finding aligns with the observations of Butnan et al. (2015), Burrell et al. (2016), and Patwa et al. (2024). An increase in EC (reduction in electrical resistivity) in concrete was also reported by Şimşek (2020) with the addition of 3% BHET. The increased EC with polymer content is due to the improvement in the packaging of soil. Furthermore, functional groups such as hydroxyl (−OH) and carbonyl (C = O) in BHET interact with water molecules, releasing or attracting ions. These interactions increase the concentration of free ions in solution, further contributing to a rise in EC. Thus, the synergistic effect of both the polymer and biochar increases the availability and mobility of charge carriers (i.e., ions in water), leading to a significant increase in EC.

3.5. Correlation between suction and electrical conductivity

Figures 10*a*–10*c* represents the relationship between suction and EC for SCM composites containing different biochar contents with (a) 0% BHET, (b) 2% BHET, and (c) 3% BHET polymer. This relationship is best described by a sigmoidal model as represented by eq. 8, with a high coefficient of determination ($R^2 > 0.95$). In eq. 8, the EC ($f(x)$) is expressed as a function of suction (x), with the corresponding fitting parameters summarized in Table 6.

$$f(x) = d + (a - d)\, e^{-e^{-b(x-c)}} \quad (8)$$

where, a = upper asymptote of EC, d = lower asymptote of EC, b = growth rate parameter, and c = inflection point of curve.

As seen in Figs. 10*a*–10*c*, a nonlinear decline in EC with increasing suction is observed, reflecting the reduction in water-filled conductive pathways as soils dry. Similarly, samples with higher biochar %, for instance, SCM-25B-0P, retain higher EC at higher suction levels, which can be attributed to improved water retention (Kibria and Hossain 2015) and enhanced pore connectivity (Burrell et al. 2016). In Fig. 10*b*, the introduction of 2% BHET polymer further improves conductivity. Figure 10*c* shows that the addition of 3% BHET polymer further improves the conductivity of SCM composites, exhibiting the highest EC over a broad range of suction levels, highlighting the synergistic impact of biochar and polymer in maintaining soil microstructural stability.

These improved outcomes have essential implications for hydraulic barrier applications. The higher EC at higher suction levels suggests sustained water-filled connectivity and ionic transport, which are vital in maintaining the hydraulic integrity of landfill liners under desiccating field conditions (Daniel and Benson 1990; Albrecht and Benson 2001). Biochar improves water retention, Figs. 4*a*–4*c* and EC, Figs. 9*a*–9*c*, while BHET polymer treatment further stabilizes soil microstructure, and hence reduces the risk of desiccation-induced shrinkage, cracking, and loss of barrier performance (Kou et al. 2021; Gopakumar and Bharat 2025). This combined effect of biochar and BHET polymer suggests that BHET polymer-treated biochar-amended soil can function as more durable and resilient landfill liners, ensuring long-term improved performance even under fluctuating moisture conditions (Rowe 2001).

3.6. Correlation between void ratio and electrical conductivity

Figures 11*a*–11*c* represents the relationship of EC and void ratio for the SCM composites with different biochar contents, with (a) 0% BHET polymer, (b) 2% BHET polymer, and (c) 3% BHET polymer. In all cases, EC increases with void ratio, reflecting enhanced pore connectivity. The SCM composites with higher biochar content, i.e., 25% biochar, consistently show higher EC values across the given void ratio range (Fig. 11*a*). The addition of the BHET polymer further increases

Fig. 9. Effect of degree of saturation on the electrical conductivity of soil–clay mixture (SCM) at (*a*) 0% bis(2-hydroxyethyl) terephthalate (BHET), (*b*) 2% BHET, (*c*) 3% BHET, and (*d*) electrical conductivity of the samples at optimum moisture content.

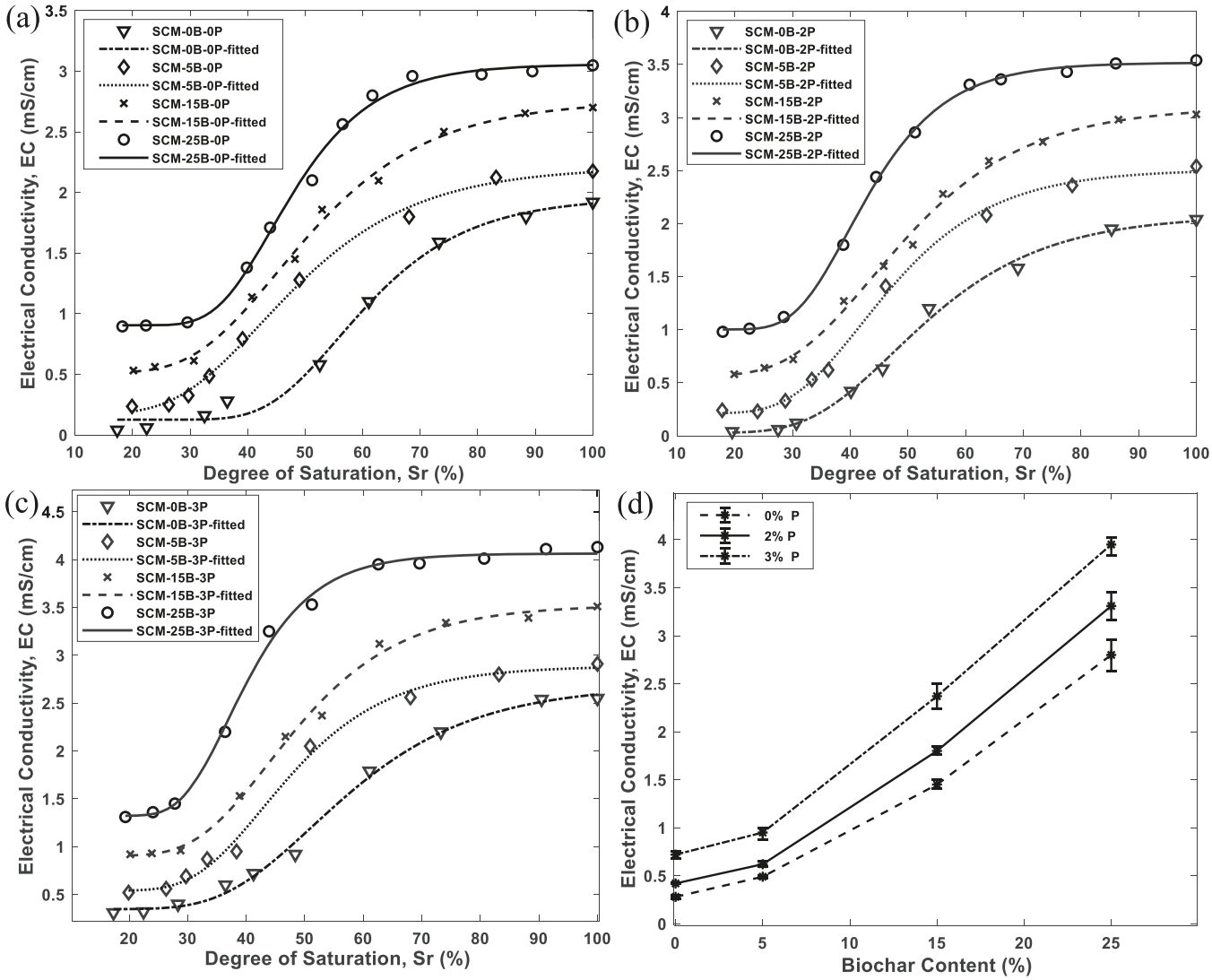

conductivity, with 3% BHET (3P), suggesting a higher EC response (Fig. 11*c*). This finding highlights the synergistic effect of biochar and the BHET polymer in maintaining conductive pathways under varying void ratios.

The relationship between EC and void ratio shows a consistent trend of increasing conductivity with increasing void ratio, due to the continuity of water-filled pores and improved ionic mobility. A similar trend of correlations has been reported in clayey soils, in which the EC is strongly influenced by pore geometry and fluid continuity (Kozaki et al. 1998; Samouëlian et al. 2005). In Fig. 11*a*, this effect is pronounced with SCM-25B-0P having the highest EC, which can be attributed to the enhanced porosity and surface charge contributions of biochar, which is consistent with previous documented literature findings that biochar addition facilitates ion transport in compacted soils (Butnan et al. 2015; Burrell et al. 2016; Patwa et al. 2024). The addition of 2% BHET polymer resulted in a steeper EC increment with void ratio, especially in SCM with a higher biochar percentage. This result suggests that the biochar and polymer interactions strengthen the conductive networks as the soil structure becomes more open due to the biochar. Similarly, for SCM composites with 3% BHET polymer, the influence is most significant, Fig. 11*c*, with SCM-25B-3P maintaining the highest EC across the given range of void ratios. This can be attributed to the synergistic stabilization of pore networks by biochar and polymer.

3.7. Unconfined compressive strength

Figures 12*a* and 12*b* show the UCS values of the SCM composites, which were cured for 1 day and 28 days, respectively. As illustrated in Fig. 12*a*, the UCS of the SCM composites decreased with the addition of biochar at 0%, 5%, 15%, and 25% after 1 day of curing. The UCS decreased by approximately 0.5%, 13%, 15.5%, and 54%, respectively. This reduction in UCS with increasing biochar content is consistent with the result documented by Jyoti Bora et al. (2021), who also observed a decline in soil UCS strength after biochar amendments. The decrease in UCS strength is primarily attributed to the reduc-

Fig. 10. Correlations between suction and electrical conductivity of soil–clay mixture (SCM) at (*a*) 0% bis(2-hydroxyethyl) terephthalate (BHET), (*b*) 2% BHET, and (*c*) 3% BHET.

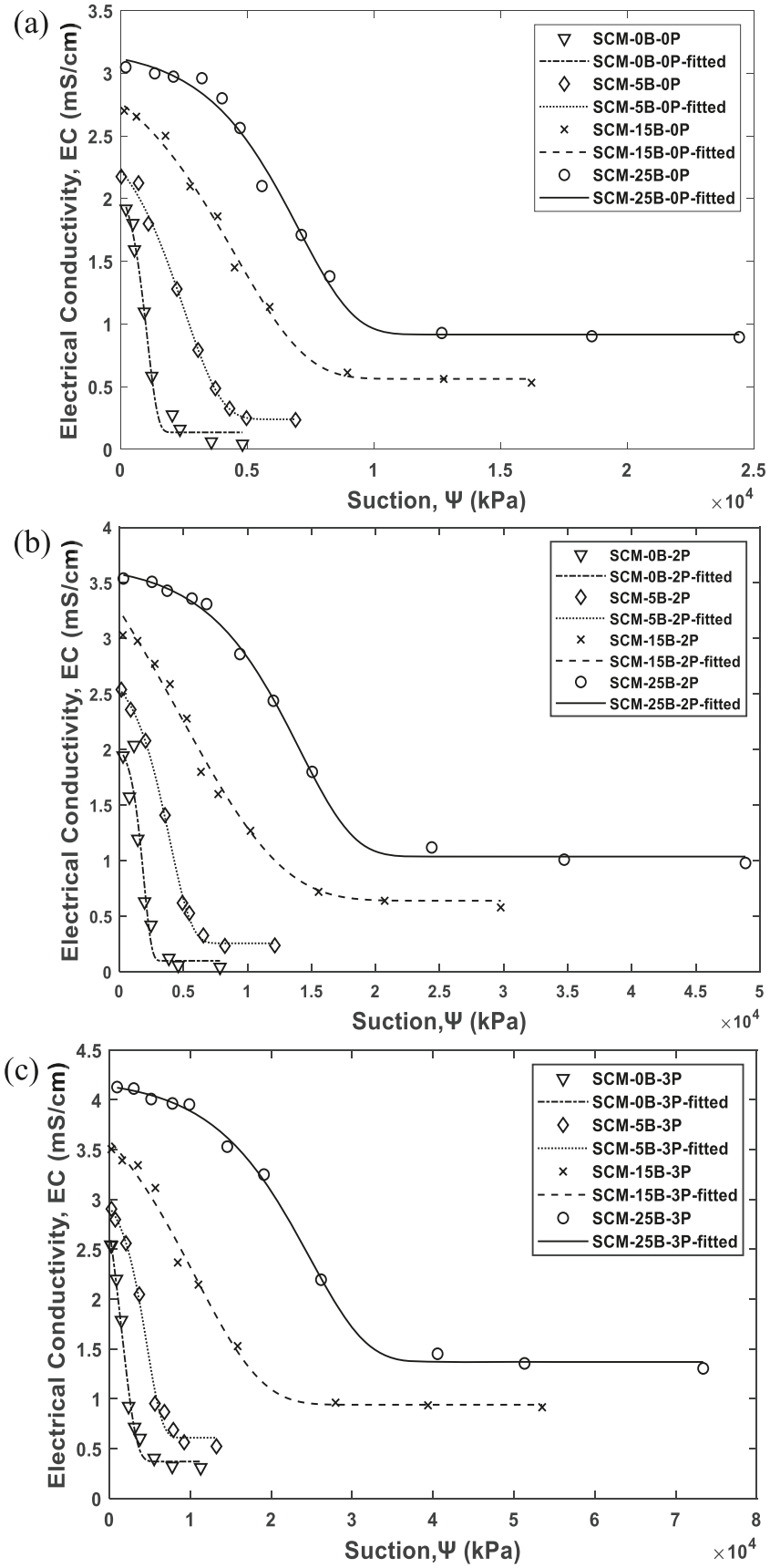

Table 6. Fitting parameters for electrical conductivity and suction correlation.

Specimen	Fitting parameters				R^2
	a	*b*	*c*	*d*	
SCM-0B-0P	2.21	− 2.40E-03	1056.00	0.14	0.99
SCM-5B-0P	2.63	− 6.77E-04	2512.40	0.24	0.99
SCM-15B-0P	3.25	− 3.56E-04	4536.10	0.56	0.99
SCM-25B-0P	3.20	− 4.59E-04	7037.00	0.92	0.99
SCM-0B-2P	2.09	− 1.60E-03	1915.40	0.10	0.95
SCM-5B-2P	2.79	− 5.78E-04	2932.80	0.26	0.99
SCM-15B-2P	5.18	− 1.25E-04	4738.60	0.64	0.98
SCM-25B-2P	3.67	− 2.35E-04	14050.00	1.04	0.99
SCM-0B-3P	3.93	− 5.37E-04	1520.90	0.37	0.99
SCM-5B-3P	3.13	− 5.30E-03	4647.50	0.61	0.99
SCM-15B-3P	4.45	− 1.21E-04	10569.00	0.94	0.99
SCM-25B-3P	4.32	− 1.27E-04	24300.00	1.38	0.99

Note: SCM, soil–clay mixture.

tion in the composite's dry density, resulting from the low specific gravity and high porosity of biochar. However, after 28 days of curing, as shown in Fig. 12*b*, the UCS of the SCM composite with 5% biochar was observed to be 9.5% higher than that of the control SCM sample without biochar. This increase in UCS is attributed to the enhanced particle interlocking of clay with biochar and increased internal friction of the SCM and biochar matrix (Sudhakar et al. 2017). Similarly, UCS of the soil significantly increased upon stabilization with BHET polymer. The UCS values steadily increased, from 452.97 to 546.83 kPa and 615.03 kPa, with the addition of 2% and 3% BHET polymer, respectively, for 1-day curing.

A similar trend is observed in the UCS result for 28 days of curing as well (Fig. 12*b*). This increment in strength is primarily attributed to the formation of interparticle bridges, hydrogen bonding, and the development of cohesive forces between the BHET polymer and the electrically charged clay particles. Additionally, after a 28-day curing period, the BHET polymer hydrogel dehydrates, becomes dense, and becomes mechanically strong. This contributes to the enhanced strength and structural integrity of the soil matrix (Fatehi et al. 2021; Ramachandran et al. 2021). The overall strengthening of the samples with BHET polymer is attributed to mechanisms such as pore filling, particle coating, and soil particle bridging (Chang et al. 2020), as well as the conglomeration and aggregation of soil grains (Patwa et al. 2024). Moreover, Chandra and Siddiqua (2022) recently reported the formation of a novel cementitious binder in a sand–bentonite (75:25) mixture stabilized with BHET polymer. This binder formation has resulted from a network of hydrogel that bridges and interlocks the soil grains together, as well as hydrogen bonding interactions between the carboxylic and hydroxyl functional groups of BHET and the clay minerals. Since the SCM used in this research also consists of a soil–bentonite clay mix, similar mechanisms may be contributing to the increased mechanical strength. Most of the SCM composites gained either increased or comparable strength, except for SCM-0B-3P and SCM-5B-3P. However, exceptions were observed for SCM-0B-3P and SCM-5B-3P, as depicted in Figs. 12*a* and 12*b*, where a decrease in UCS was observed when 3% BHET polymer was incorporated instead of 2%. This decline in strength for SCM-0B-3P and SCM-5B-3P is likely attributed to the soft, viscoelastic property of the hydrated BHET polymer. As polymer content increases, the formation of a polymer film at soil–biochar and biochar–biochar interfaces may reduce the interparticle friction and, as a result, the UCS strength of the composites can decrease (Patwa et al. 2024). Despite this, all SCM–biochar composite samples amended with BHET polymer exhibited higher UCS values than their counterparts without polymer treatment. This increase in strength is attributed to the combined effects of particle aggregation and interparticle bridging between soil and biochar, along with electrostatic adhesion of clay particles to the BHET polymer, as reported in previous studies (Fatehi et al. 2021; Ramachandran et al. 2021; Patwa et al. 2024).

When BHET polymer was added to SCM, as shown in Figs. 12*a* and 12*b*, the UCS for 1-day and 28-days increased significantly. Due to lightweight, porous, and brittle nature of biochar, it alone provides limited cementation and increases in UCS with curing time are generally modest. In this study, the observed increase in UCS for 28-days samples is mainly attributed to the clay matrix and its interaction with the BHET polymer. With increased curing time, the polymer hydrogel gradually dehydrates, forming a denser and mechanically stronger network, which enhances interparticle bonding and contributes to improved UCS values (Ramachandran et al. 2021; Vydehi and Moghal 2022).

3.8. Scanning electron microscopy

Figures 13*a*–13*f* illustrate the SEM analysis of the test samples. Results indicate an interaction mechanism among BHET, biochar, and soil. Figure 13*a* illustrates SCM with biochar characterized by open voids, in contrast to the polymer-treated soils of Fig. 13*c*. Figures 13*b* and 13*d* report SEM images of SCM samples with biochar and BHET, where the biochar particles are uniformly dispersed throughout the clay matrix, while BHET polymer encapsulates the soil particles. Figure 13*e* shows the flocculation of bentonite clay and the formation of a "card-house" structure. This is caused by the combination of electrostatic forces, ion–dipole, and dipole–dipole (hydrogen bonding) interactions. Comparable flocculated clay structures have been reported in previous studies that examined the interaction of anionic polymers with clay materials; for instance, a BHET polymer-treated SBM (Chandra and Siddiqua 2022) and plastic silt treated with XG (Singh and Das 2020). Figure 13*f* depicts the layered architecture of the BHET polymer, which appears to maintain the integrity of the clay clusters and may contribute to enhanced water retention and resistance to shrinkage and swelling. A polymer coating is observed on soil and biochar, which is likely attributed to hydrogen bonding between water molecules and hydroxyl groups present in the BHET structure. Chandra and Siddiqua (2022) documented comparable results by combining the BHET polymer with the SBM.

Fig. 11. Correlations between void ratio and electrical conductivity of soil–clay mixture (SCM) at (*a*) 0% bis(2-hydroxyethyl) terephthalate (BHET), (*b*) 2% BHET, and (*c*) 3% BHET.

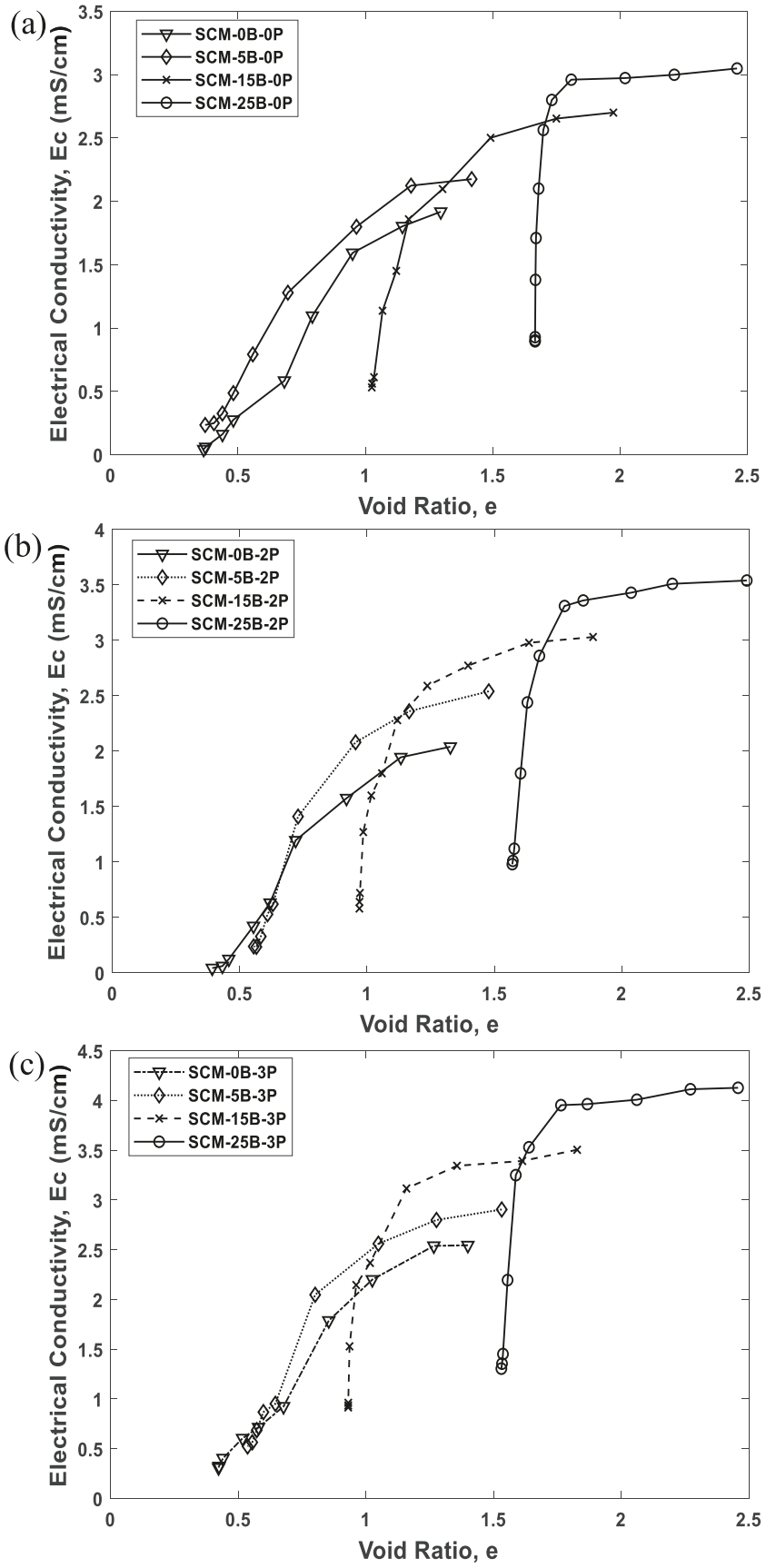

Fig. 12. Unconfined compressive strength (UCS) of soil–clay mixture (SCM) samples after (*a*) 1-day curing and (*b*) 28-days curing.

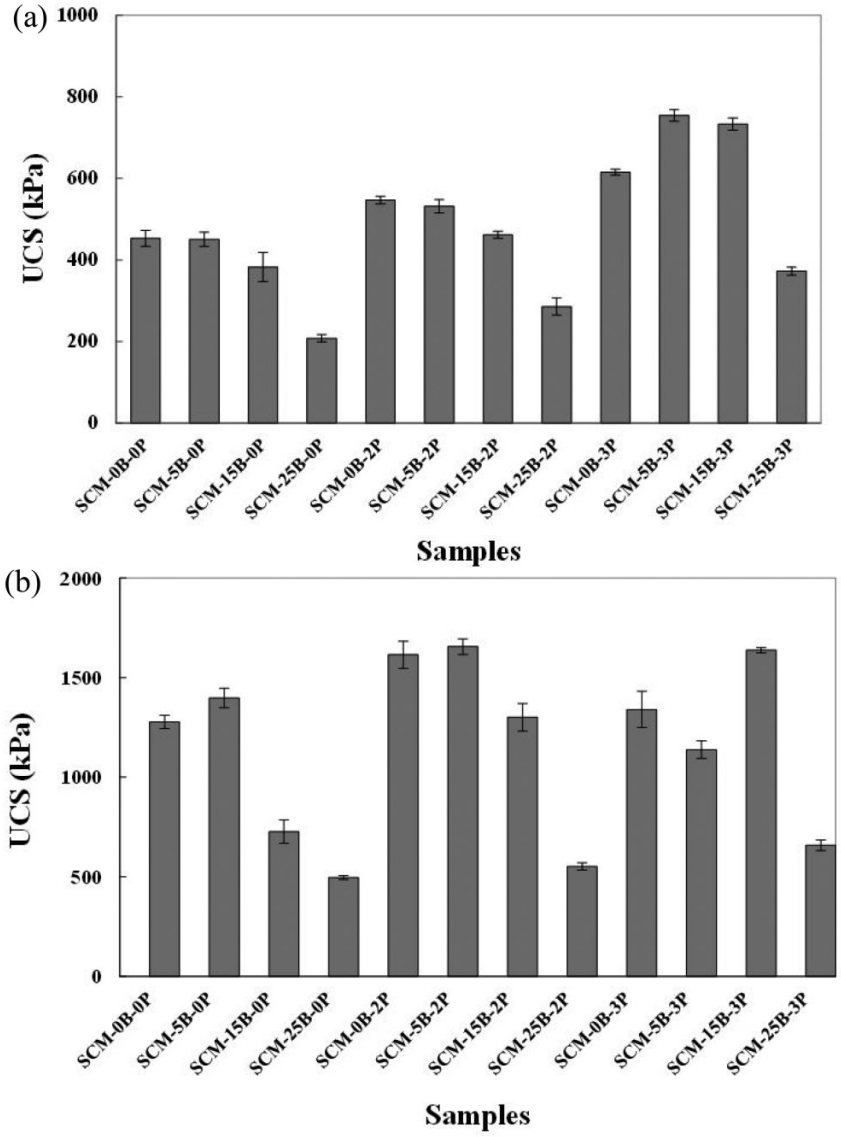

The elemental peaks found in spectrum 6 and spectrum 7, as shown in Fig. 14, support the existence of carbon (C), oxygen (O), and silicon (Si) as primary elements, and iron (Fe), aluminum (Al), sodium (Na), and others as minor elements. The presence of the BHET polymer, i.e., $C_{12}H_{14}O_6$, is validated by the strong peaks of O and C (Chandra and Siddiqua 2022). Moreover, the presence of Si, O, Al, Na, and Fe supports the presence of clay/soil within the BHET polymer matrix. Similarly, the peak at C in Fig. 14 corresponds to biochar in the composite samples. These results together support the interaction and the bonding hypothesis for BHET polymer, biochar, and the clay, and suggest the integration at the microstructural level.

4. Potential engineering applications

The applications of BHET polymer and biochar in soil stabilization could well be realized in various geotechnical works, especially where enhanced water retention, reduced shrinkage, and adequate strength are required. The most common areas of application would relate to hydraulic barriers in waste disposal facilities, where maintaining structural integrity while controlling shrinkage and desiccation cracking is critical. The use of low dosages of polymers with biochar-amended soil provides a potentially sustainable alternative to conventional stabilization methods. A representative operating procedure for polymer-stabilized biochar-amended soil liners is illustrated in Fig. 15 and comprises polymer spreading, mechanical mixing, moisture conditioning, compaction, and preparation of the stabilized liner surface. consistent with standard liner construction practices.

Beyond landfill applications, the method can be suitable to canal linings, erosion control layers, and other low-permeability barriers. However, further field-scale studies at full scale are recommended to investigate its long-term performance and durability.

Fig. 13. Scanning electron microscopy for biochar- and bis(2-hydroxyethyl) terephthalate-treated soil–clay mixture (SCM): (*a*) biochar and clay binding, (*b*) polymer coating on biochar, (*c*) polymer intact soil, (*d*) polymer lumps swelled in between soil and biochar grains, (*e*) flocculation of bentonite in SCM matrix, and (*f*) polymer hydrogel filling voids.

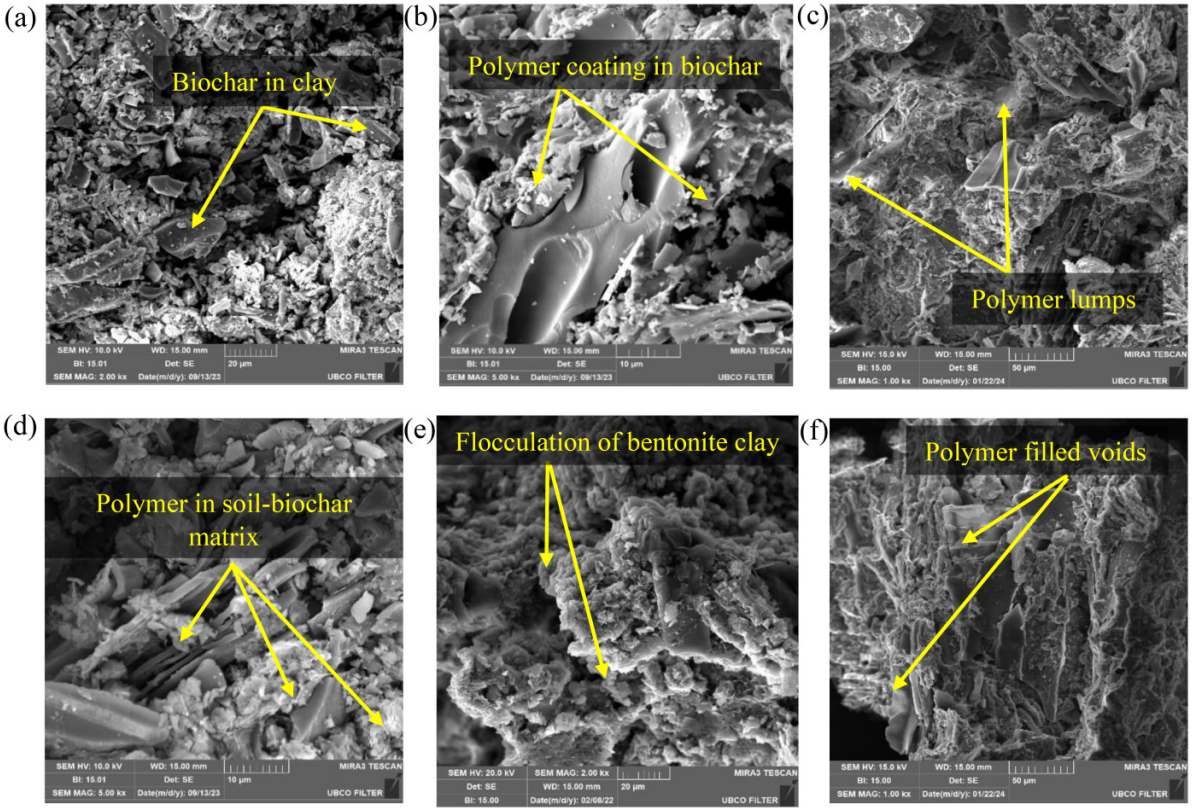

Fig. 14. Scanning electron microscopy image and EDS analysis showing elemental peaks for different elements. SCM, soil–clay mixture.

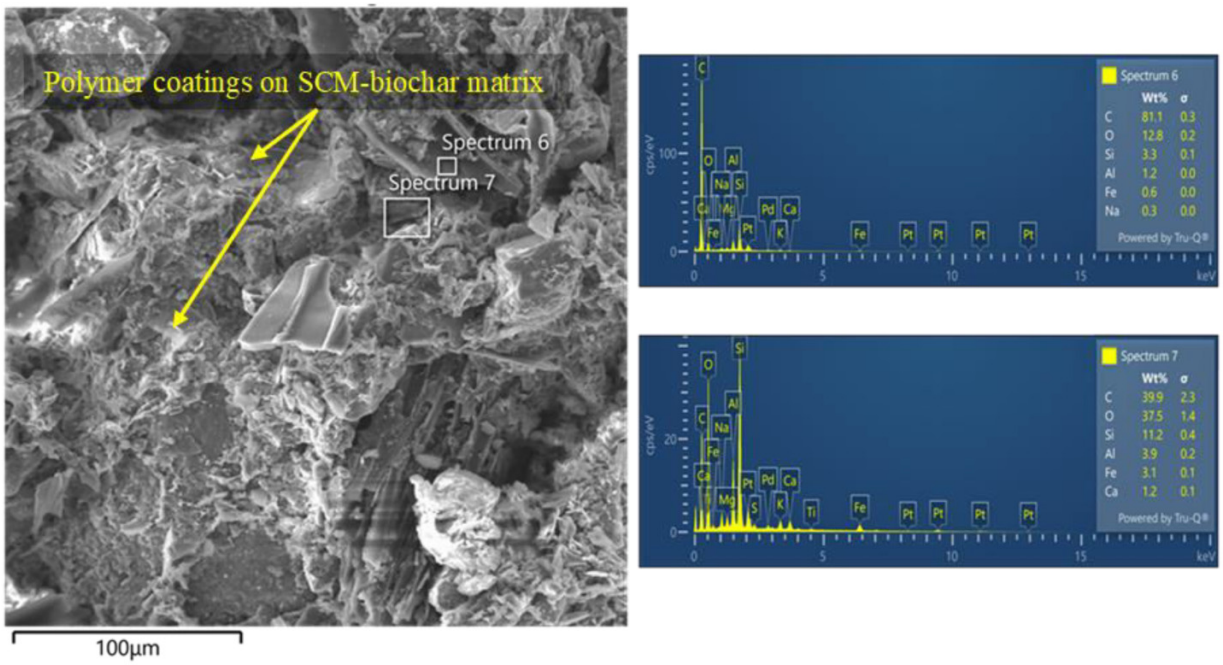

Fig. 15. Schematic illustration of a representative field-scale operating procedure for the application of bis(2-hydroxyethyl) terephthalate polymer for soil stabilization.

5. Conclusion

An experimental investigation was conducted on locally sourced silty sand soil modified with clay, biochar, and BHET polymer to assess alterations in essential attributes, including water retention capacity, shrinkage potential, and EC. The practicality of these combinations for geotechnical and geoenvironmental purposes was examined, leading to the following main conclusions:

1. Both BHET polymer and biochar can significantly enhance soil water holding capacity, as evidenced by prior studies and the findings of this research. This increased moisture retention effectively contributes to shrinkage control in liner soil, attributed to the polymerization of the BHET polymer hydrogel, biochar, and soil particles.
2. The AEV of the composites increased with the addition of biochar and polymer, while volumetric shrinkage was significantly reduced. These findings suggest that liners with improved AEV are more effective at controlling shrinkage and volumetric changes, which are essential to maintaining the long-term operational quality of the liner. Moreover, establishing an elevated AEV helps delay desaturation, thereby enhancing the stability of landfill liners and improving their overall performance.
3. The addition of BHET polymer to bare SCM at 2% and 3% resulted in a rise in e_{min}, roughly by 4.5% and 16.5%, respectively. A significant rise in e_{min} was also observed in samples with biochar amendments only. However, a reduction in e_{min} was observed when BHET was introduced into biochar-amended SCM, suggesting an interaction between the polymer and biochar within the soil matrix. This indicates that a higher polymer concentration mitigates the alteration in void ratio induced by biochar treatment.
4. The void ratio for soil–biochar–polymer mixes exhibits an inverse correlation with suction ($R^2 > 0.95$), which offers a practical and straightforward approach for estimating the preliminary suction values of the samples. This relationship helps regulate volumetric changes, moisture retention, and the overall mechanical properties of the soil.
5. The EC of the samples increased with higher water content, as higher saturation improves particle bridging and enhances charge mobility by releasing adsorbed charges. Similarly, the EC of SCM increases with the addition of polymer and biochar, as polymers act as binding agents, enhancing soil–biochar interactions and reducing parti-

cle spacing through closer packing. Additionally, the hydrogel viscosity and polymer–clay interactions, including cation bridging, enhance the microstructural stability of soil. This stabilized structure improves the continuity of conduction pathways, resulting in higher EC in the polymer–biochar–soil composite.

6. Among all the SCM composite samples that were tested, the UCS of the SCM composite with 2% BHET polymer and 5% biochar had the highest value. The improvement in strength is attributed to the interaction among the biochar, BHET polymer, and clay/soil particles, which increases bonding and cohesion among them and thereby enhances the structural strength of the SCM matrix.
7. SEM analysis of BHET-treated specimens suggests clay flocculation, the polymer-mediated bridging between biochar and soil, and the presence of polymer–biochar–soil associations.

This study emphasizes the potential of the BHET polymer and biochar as novel stabilizers to enhance the shrinkage resistance and moisture retention of CCLs. The findings suggest that an interaction mechanism exists between the polymer and biochar at the microstructural level as well. Derived from discarded PET bottles, BHET offers the key benefit of improving liner performance in high-moisture environments, such as landfill liners. This approach not only addresses civil engineering challenges but also contributes to effective waste management by diverting PET waste from landfills. Although BHET is non-biodegradable, its long-term stability in soil environments is not yet fully understood. Therefore, future studies should focus on field-scale validation and long-term durability assessments to better evaluate both environmental sustainability and engineering performance.

Acknowledgements

The corresponding author acknowledges the funding support from the Natural Sciences and Engineering Research Council of Canada (NSERC)/Discovery Grants Program (Grant # 62R09724). The authors also acknowledge the Fipke Laboratory for Trace Element Research at the University of British Columbia's Okanagan campus for providing the opportunity to conduct microscopic examinations.

Article information

History dates

Received: 19 November 2025
Accepted: 10 February 2026
Version of record online: 25 March 2026

Copyright

Data availability

All data, models, and code generated or used during the study appear in the published article.
Data will be made available on request.

Author information

Author ORCIDs

Sumi Siddiqua https://orcid.org/0000-0002-3808-0670

Author notes

Sumi Siddiqua served as Associate Editor at the time of manuscript review and acceptance; peer review and editorial decisions regarding this manuscript were handled by another editorial board member.

Author contributions

Conceptualization: SS, AC
Data curation: UA
Formal analysis: UA
Funding acquisition: SS
Investigation: UA
Methodology: UA, AC
Project administration: SS
Resources: SS
Supervision: SS
Validation: AC
Visualization: AC
Writing – original draft: UA
Writing – review & editing: SS, AC

References

Al-Taie, A.J., Al-Obaidi, A., and Alzuhairi, M. 2020. Utilization of depolymerized recycled polyethylene terephthalate in improving poorly graded soil. Transportation Infrastructure Geotechnology, **7**(2): 206–223. doi:10.1007/s40515-019-00099-2.

Albrecht, B.A., and Benson, C.H. 2001. Effect of desiccation on compacted natural clays. Journal of Geotechnical and Geoenvironmental Engineering, **127**(1): 67–75. doi:10.1061/(ASCE)1090-0241(2001)127:1(67).

Alonso, E.E., Gens, A., and Josa, A. 1990. A constitutive model for partially saturated soils. Géotechnique, **40**(3).

Alves de Godoy Leme, M., and Gonçalves Miguel, M. 2018. Permeability and retention to water and leachate of a compacted soil used as liner. Water, Air, & Soil Pollution, **229**(11). doi:10.1007/s11270-018-4001-0.

Andrew, R.M. 2019. Global CO2 emissions from cement production, 1928–2018. In Earth System Science Data **11**(4): 1675–1710. Copernicus GmbH. doi:10.5194/essd-11-1675-2019.

Arnold, S.L., Doran, J.W., Schepers, J., Wienhold, B., Ginting, D., Amos, B., and Gomes, S. 2005. Portable probes to measure electrical conductivity and soil quality in the field. Communications in Soil Science and Plant Analysis, **36**(15–16): 2271–2287. doi:10.1080/00103620500196689.

ASTM D-2166. 2006. Standard test method for unconfined compressive strength of cohesive soil.

ASTM D698. 2012. Standard Test Methods for Laboratory Compaction Characteristics of Soil Using Standard Effort (12 400 ft-lbf/ft^3 (600 kN-m/m^3)).

ASTM, D. 4. 0. 2017. Standard test methods for liquid limit, plastic limit, and plasticity index of soils. ASTM International, West Conshohocken.

ASTM. 2011. Standard practice for classification of soils for engineering purposes (Unified Soil Classification System) 1. ASTM International, West Conshohocken. doi:10.1520/D2487-11.

ASTM. 2019. Standard test methods for pH of Soils. ASTM, West Conshohocken, 19.

Bai, W., Zhang, H., Liu, B., Wu, Y., and Song, J.Q. 2010. Effects of superabsorbent polymers on the physical and chemical properties of soil following different wetting and drying cycles. Soil Use and Management, **26**(3): 253–260. doi:10.1111/j.1475-2743.2010.00271.x.

Bhardwaj, A.K., McLaughlin, R.A., Shainberg, I., and Levy, G.J. 2009. Hydraulic characteristics of depositional seals as affected by exchangeable cations, clay mineralogy, and polyacrylamide. Soil Science Society of America Journal, **73**(3): 910–918. doi:10.2136/sssaj2007.0426.

Bhurtel, A., Salifu, E., and Siddiqua, S. 2024. Composite biomediated engineering approaches for improving problematic soils: potentials and opportunities. Science of The Total Environment, **914**(169808): 169808. doi:10.1016/j.scitotenv.2023.169808.

Burrell, L.D., Zehetner, F., Rampazzo, N., Wimmer, B., and Soja, G. 2016. Long-term effects of biochar on soil physical properties. Geoderma, **282**: 96–102. doi:10.1016/j.geoderma.2016.07.019.

Butnan, S., Deenik, J.L., Toomsan, B., Antal, M.J., and Vityakon, P. 2015. Biochar characteristics and application rates affecting corn growth and properties of soils contrasting in texture and mineralogy. Geoderma, **237**: 105–116.

Cai, W., Bordoloi, S., Ng, C.W.W., and Sarmah, A.K. 2022. Influence of pore fluid salinity on shrinkage and water retention characteristics of biochar amended kaolin for landfill liner application. Science of The Total Environment, **838**: 156493. doi:10.1016/j.scitotenv.2022.156493.

Castaño, V.M., Castaño, C., Alvarez-Castillo, A., VázquezvávázquezPolo, G., Acosta, D., González, V., and González, G. 1998. High resolution electron microscopy of bis-(-2-Hydroxyethyl) terephthalate crystalline polymers. Microscopy Research and Technique, **40**: 41–48. doi:10.1002/(SICI)1097-0029(19980101)40:1⟨41::AID-JEMT6⟩3.0.CO;2.

Chandra, A., and Ravi, K. 2020. Effect of magnesium incorporation in enzyme-induced carbonate precipitation (EICP) to improve shear strength of soil. *In* Lecture Notes in Civil Engineering. Springer, Singapore. pp. 333–346. doi:10.1007/978-981-15-0890-5_28.

Chandra, A., and Ravi, K. 2021. Application of enzyme-induced carbonate precipitation (EICP) to improve the shear strength of different type of soils. *In* Lecture Notes in Civil Engineering. Springer, Singapore. pp. 617–632. doi:10.1007/978-981-15-6237-2_52.

Chandra, A., and Siddiqua, S. 2022. A novel application of bis (2-Hydroxyethyl) terephthalate to enhance sand bentonite mixture for landfills. Journal of Materials in Civil Engineering, **34**(9):. doi:10.1061/(ASCE)MT.1943-5533.0004341.

Chandra, A., and Siddiqua, S. 2023. Sustainable utilization of chemically depolymerized polyethylene terephthalate (PET) waste to enhance sand-bentonite clay liners. Waste Management, **166**: 346–359. doi:10.1016/j.wasman.2023.04.030.

Chang, I., Lee, M., Tran, A.T.P., Lee, S., Kwon, Y.M., Im, J., and Cho, G.C. 2020. Review on biopolymer-based soil treatment (BPST) technology in geotechnical engineering practices. Transportation Geotechnics, **24**: 100385. doi:10.1016/j.trgeo.2020.100385.

Chen, P., and Lu, N. 2018. Generalized equation for soil shrinkage curve. Journal of Geotechnical and Geoenvironmental Engineering **144**(8): 04018046. doi:10.1061/(asce)gt.1943-5606.0001889.

Chen, Z., Luo, P., and Fu, Q. 2009. Preparation and properties of organomodifier free PET/MMT nanocomposites via monomer intercalation and in situ polymerization. Polymers for Advanced Technologies, **20**(12): 916–925. doi:10.1002/pat.1336.

Chertkov, V.Y. 2000. Modeling the pore structure and shrinkage curve of soil clay matrix. Geoderma, **95**: 215–246. doi:10.1016/S0016-7061(99)00087-7.

Daniel, D.E., and Benson, C.H. 1990. Water content-density criteria for compacted soil liners. Journal of Geotechnical Engineering, **116**(12): 1811–1830. doi:10.1061/(ASCE)0733-9410(1990)116:12(1811).

Daniel, D.E., and Koerner, R.M. 1993. Quality assurance and quality control for waste containment facilities. Cincinnati: Risk Reduction Engineering Laboratory, Office of Research and Development, US Environmental Protection Agency.

de F. N. Gitirana, G., and Fredlund, D.G. 2004. Soil–water characteristic curve equation with independent properties. Journal of Geotechnical and Geoenvironmental Engineering, **130**(2): 209–212. doi:10.1061/(ASCE)1090-0241(2004)130:2(209).

Dong, C., Guo, Z., Zhu, Y., Rui, S., and Li, Y. 2025. Effect of water glass-enhanced biocementation in sand: early strength enhancement and mechanistic insights. Construction and Building Materials, **479**: 141516. doi:10.1016/j.conbuildmat.2025.141516.

Fatehi, H., Ong, D.E.L., Yu, J., and Chang, I. 2021. Biopolymers as green binders for soil improvement in geotechnical applications: a review. Geosciences, **11**(7): 291. doi:10.3390/geosciences11070291.

Fatima, N., Zhang, Q., Chen, R., Yan, D., Zhou, Q., Lu, X., and Xin, J. 2020. Adsorption thermodynamics and kinetics of resin for metal impurities in bis(2-hydroxyethyl) terephthalate. Polymers, **12**(12): 1–12. doi:10.3390/polym12122866.

Fredlund, D.G., and Rahardjo, H. 1993. Soil mechanics for unsaturated soils. John Wiley & Sons, 517. doi:10.1002/9780470172759.

Fredlund, M.D., Wilson, G.W., and Fredlund, D.G. 2002. Representation and estimation of the shrinkage curve. *In* Proceedings of the 3rd International Conference on Unsaturated Soils, Recife, Brazil. Available from https://hdl.handle.net/1783.1/13621 [accessed October 2025].

Garg, A., Bordoloi, S., Ni, J., Cai, W., Maddibiona, P.G., Mei, G., et al. 2019. Influence of biochar addition on gas permeability in unsaturated soil. Géotechnique Letters, **9**(1): 66–71. doi:10.1680/jgele.18.00190.

Gopakumar, V., and Bharat, V.T. 2025. A novel biopolymer-amended bentonite-based capillary barrier: performance evaluation against rainfall-induced landslides. Canadian Geotechnical Journal, **62**: 1–26. doi:10.1139/cgj-2024-0715.

Heaney, M.B. 2003. Electrical conductivity and resistivity. Electrical Measurement, Signal Processing, and Displays, **7**(1).

Hernández, M.A., Elizondo, P., Sánchez, M.G., Pérez, N.A., Elizalde, L.E., and Rivas, B.L. 2015. Degraded pet for the removal of metal ions from aqueous solution. Journal of the Chilean Chemical Society, **60**.

Jing, F., Sun, Y., Liu, Y., Wan, Z., Chen, J., and Tsang, D.C.W. 2022. Interactions between biochar and clay minerals in changing biochar carbon stability. Science of The Total Environment, **809**: 151124. doi:10.1016/j.scitotenv.2021.151124.

Jyoti Bora, M., Bordoloi, S., Kumar, H., Gogoi, N., Zhu, H.-H., Sarmah, A.K., et al. 2021. Influence of biochar from animal and plant origin on the compressive strength characteristics of degraded landfill surface soils. International Journal of Damage Mechanics, **30**(4): 484–501. doi:10.1177/1056789520925524.

Kalinski, R., and Kelly, W. 1993. Estimating water content of soils from electrical resistivity. Geotechnical Testing Journal, **16**(3): 323–329. doi:10.1520/GTJ10053J.

Khan, V., Roy, S., and Rajesh, S. 2022. Numerical investigation on hydraulic and gas flow response of MSW landfill cover system comprising a geosynthetic clay liner under arid climatic conditions. Geotextiles and Geomembranes, **50**(6): 1159–1171. doi:10.1016/j.geotexmem.2022.08.001.

Kibria, G., and Hossain, M.S. 2012. Investigation of geotechnical parameters affecting electrical resistivity of compacted clays. Journal of Geotechnical and Geoenvironmental Engineering, **138**(12): 1520–1529. doi:10.1061/(ASCE)GT.1943-5606.0000722.

Kibria, G., and Hossain, M.S. 2015. Investigation of degree of saturation in landfill liners using electrical resistivity imaging. Waste Management, **39**: 197–204. doi:10.1016/j.wasman.2015.02.015.

Kou, H., Jia, H., Chu, J., Zheng, P., and Liu, A. 2021. Effect of polymer on strength and permeability of marine clay. Marine Georesources & Geotechnology, **39**(2): 234–240. doi:10.1080/1064119X.2019.1693669.

Kozaki, T., Fujishima, A., Sato, S., and Ohashi, H. 1998. Self-diffusion of sodium ions in compacted sodium montmorillonite. Nuclear Technology, **121**(1): 63–69. doi:10.13182/NT98-A2819.

Li, J.H., Li, L., Chen, R., and Li, D.Q. 2016. Cracking and vertical preferential flow through landfill clay liners. Engineering Geology, **206**: 33–41. doi:10.1016/j.enggeo.2016.03.006.

Li, Y., Guo, Z., Wang, L., Zhu, Y., and Rui, S. 2024. Field implementation to resist coastal erosion of sandy slope by eco-friendly methods. Coastal Engineering, **189**: 104489. doi:10.1016/j.coastaleng.2024.104489.

Li, Y., Li, Y., Guo, Z., and Xu, Q. 2023. Durability of MICP-reinforced calcareous sand in marine environments: laboratory and field experimental study. Biogeotechnics, **1**(2): 100018. doi:10.1016/j.bgtech.2023.100018.

Lima, A.N., Silva, T.F., Silva, D.L.M., Silvani, C., Monteiro, V.E.D., and Melo, M.C. 2026. Soil-contaminant interaction in silty sand-bentonite

liners percolated by landfill leachate. International Journal of Environmental Science and Technology, **23**(1). doi:10.1007/s13762-025-06952-x.

Little, D., and Nair, S. 2009. Recommended practice for stabilization of subgrade soils and base materials. National Cooperative Highway Research Program, Transportation Research Board of the National Academies, USA. Google Scholar. pp. 1–30.

Liu, J., Wang, Y., Lu, Y., Feng, Q., Zhang, F., Qi, C., et al. 2017. Effect of polyvinyl acetate stabilization on the swelling-shrinkage properties of expansive soil. International Journal of Polymer Science, **2017**: 1–8. doi:10.1155/2017/8128020.

Liu, T., and Hu, L. 2014. Organic acid transport through a partially saturated liner system beneath a landfill. Geotextiles and Geomembranes, **42**(5): 428–436. doi:10.1016/j.geotexmem.2014.06.007.

Liu, Y., Yao, X., Yao, H., Zhou, Q., Xin, J., Lu, X., and Zhang, S. 2020. Degradation of poly(ethylene terephthalate) catalyzed by metal-free choline-based ionic liquids. Green Chemistry, **22**(10): 3122–3131. doi:10.1039/D0GC00327A.

Lu, S.G., Sun, F.F., and Zong, Y.T. 2014. Effect of rice husk biochar and coal fly ash on some physical properties of expansive clayey soil (Vertisol). Catena, **114**: 37–44. doi:10.1016/j.catena.2013.10.014.

Mahamaya, M., Das, S.K., Reddy, K.R., and Jain, S. 2021. Interaction of biopolymer with dispersive geomaterial and its characterization: an eco-friendly approach for erosion control. Journal of Cleaner Production, **312**: 127778. doi:10.1016/j.jclepro.2021.127778.

Mei, G., Kumar, H., Reddy, N.G., Huang, S., Balaji, C.R., Sadasiv, S.G., and Zhu, H.-H. 2020. Evaluating suitability of geomaterials-amended soil for landfill liner: a comparative study. Journal of Hazardous, Toxic, and Radioactive Waste, **24**(4). doi:10.1061/(ASCE)HZ.2153-5515.0000551.

Moghal, A.A.B., and Vydehi, K.V. 2021. State-of-the-art review on efficacy of xanthan gum and guar gum inclusion on the engineering behavior of soils. Innovative Infrastructure Solutions, **6**(2). doi:10.1007/s41062-021-00462-8.

Narjary, B., Aggarwal, P., Singh, A., Chakraborty, D., and Singh, R. 2012. Water availability in different soils in relation to hydrogel application. Geoderma, **187–188**: 94–101. doi:10.1016/j.geoderma.2012.03.002.

Ng, C.W.W., and Pang, Y.W. 2000. Experimental investigations of the soil-water characteristics of a volcanic soil. Canadian Geotechnical Journal, **37**: 1252–1264, doi:10.1139/t00-056.

Ni, J., Li, S.S., Ma, L., and Geng, X.Y. 2020. Performance of soils enhanced with eco-friendly biopolymers in unconfined compression strength tests and fatigue loading tests. Construction and Building Materials, **263**: 120039. doi:10.1016/j.conbuildmat.2020.120039.

Öncü, Ş., and Bilsel, H. 2017. Effect of zeolite utilization on volume change and strength properties of expansive soil as landfill barrier. Canadian Geotechnical Journal, **54**(9): 1320–1330. doi:10.1139/cgj-2016-0483.

Patwa, D., Chandra, A., Ravi, K., Sreedeep, S., and Asce, M. 2021. Influence of biochar particle size fractions on thermal and mechanical properties of biochar-amended soil. Journal of Materials in Civil Engineering, **33**. doi:10.1061/(ASCE)MT.1943-5533.0003915.

Patwa, D., Dubey, A.A., Ravi, K., and Sreedeep, S. 2024. Investigation of thermal and strength characteristics of a natural backfill composite inspired by synergistic biochar–biopolymer amendment of clay loam. Canadian Geotechnical Journal, **61**(6): 1073–1093. doi:10.1139/cgj-2022-0528.

Pham, C.T., Nguyen, B.T., Nguyen, M.T., Nguyen, T.H., Hoang, C.N., Ngan Nguyen, N., et al. 2021. The advancement of bis(2-hydroxyethyl)terephthalate recovered from post-consumer poly(ethylene terephthalate) bottles compared to commercial polyol for preparation of high performance polyurethane. Journal of Industrial and Engineering Chemistry, **93**: 196–209. doi:10.1016/j.jiec.2020.09.024.

Piqué, T.M., Manzanal, D., Codevilla, M., and Orlandi, S. 2019. Polymer-enhanced soil mixtures for potential use as covers or liners in landfill systems. Environmental Geotechnics, **8**(7): 467–479. doi:10.1680/jenge.18.00174.

Pozdnyakov, A.I., Pozdnyakova, L.A., and Karpachevskii, L.O. 2006. Relationship between water tension and electrical resistivity in soils. Eurasian Soil Science, **39**(S1): S78–S83. doi:10.1134/S1064229306130138.

Qiu, L., Yin, X., Liu, T., Zhang, H., Chen, G., and Wu, S. 2020. Biodegradation of bis(2-hydroxyethyl) terephthalate by a newly isolated *Enterobacter* sp. HY1 and characterization of its esterase properties. Journal of Basic Microbiology, **60**(8): 699–711. doi:10.1002/jobm.202000053.

Ramachandran, A.L., Dubey, A.A., Dhami, N.K., and Mukherjee, A. 2021. Multiscale study of soil stabilization using bacterial biopolymers. Journal of Geotechnical and Geoenvironmental Engineering, **147**(8). doi:10.1061/(ASCE)GT.1943-5606.0002575.

Reddy, K.R., Yaghoubi, P., and Yukselen-Aksoy, Y. 2015. Effects of biochar amendment on geotechnical properties of landfill cover soil. Waste Management & Research: The Journal for a Sustainable Circular Economy, **33**(6): 524–532. doi:10.1177/0734242X15580192.

Rowe, R.K. 2001. Barrier Systems. *In* Geotechnical and Geoenvironmental Engineering Handbook. Springer US. pp. 739–788. doi:10.1007/978-1-4615-1729-0_25.

Rowe, R.K. 2011. Systems engineering: the design and operation of municipal solid waste landfills to minimize contamination of groundwater. Geosynthetics International, **18**(6): 391–404. doi:10.1680/gein.2011.18.6.391.

Saha, A., Gupt, C.B., and Sekharan, S. 2021. Recycling natural fibre to superabsorbent hydrogel composite for conservation of irrigation water in semi-arid regions. Waste and Biomass Valorization, **12**(12): 6433–6448. doi:10.1007/s12649-021-01489-9.

Salager, S., Nuth, M., Ferrari, A., and Laloui, L. 2013. Investigation into water retention behaviour of deformable soils. Canadian Geotechnical Journal, **50**(2): 200–208. doi:10.1139/cgj-2011-0409.

Samouëlian, A., Cousin, I., Tabbagh, A., Bruand, A., and Richard, G. 2005. Electrical resistivity survey in soil science: a review. Soil and Tillage Research, **83**(2): 173–193. doi:10.1016/j.still.2004.10.004.

Shen, S.Q., and Wei, M.L. 2018. Hydraulic conductivity of polymer-amended sand-bentonite backfills permeated with lead nitrate solutions. Advances in Civil Engineering, **2018**. doi:10.1155/2018/9435194.

Shin, E.C., Kang, J.K., and Lee, H.M. 2021. Applicability of recycled soil mixed with bentonite and polymer as a waste landfill liner. Indian Geotechnical Journal, **51**(3): 451–459. doi:10.1007/s40098-021-00537-4.

Şimşek, B. 2020. Bis-hydroxyethyl terephthalate cementitious composites properties: a comparative study including hydrogen bonding mechanism with the dioctyl terephthalate. Construction and Building Materials, **258**: 119691. doi:10.1016/J.CONBUILDMAT.2020.119691.

Singh, S.P., and Das, R. 2020. Geo-engineering properties of expansive soil treated with xanthan gum biopolymer. Geomechanics and Geoengineering, **15**(2): 107–122. doi:10.1080/17486025.2019.1632495.

Smitha, S., Rangaswamy, K., and Keerthi, D.S. 2021. Triaxial test behaviour of silty sands treated with agar biopolymer. International Journal of Geotechnical Engineering, **15**(4): 484–495. doi:10.1080/19386362.2019.1679441.

Su, Y., Qu, F., Meng, Y., Xu, W., Zhu, X., Zhang, C., and Tsang, D.C.W. 2024. Microbial-induced carbonate precipitation (MICP) modified biochar for low-carbon cementitious materials. Construction and Building Materials, **451**: 138644. doi:10.1016/j.conbuildmat.2024.138644.

Sudhakar, A., Remya, N., and Varghese, G.K. 2017. Estimation of effect of sugarcane bagasse biochar amendment in landfill soil cover on geotechnical properties and landfill gas emission. Environmental Quality Management, **27**(2): 33–39. doi:10.1002/tqem.21528.

Sun, W.-J., Li, M.-Y., Zhang, W.-J., and Tan, Y.-Z. 2020. Saturated permeability behavior of biochar-amended clay. Journal of Soils and Sediments, **20**: 3875–3883. doi:10.1007/s11368-020-02720-1.

Tabiatnejad, B., Siddiqua, S., and Siemens, G. 2016. Impact of pore fluid salinity on the mechanical behavior of unsaturated bentonite–sand mixture. Environmental Earth Sciences, **75**(22). doi:10.1007/s12665-016-6246-5.

Taheri, S., and El-Zein, A. 2025. Enhanced resistance to desiccation cracking of polymer–bentonite mixtures: an experimental investigation of underlying mechanisms. Canadian Geotechnical Journal, **62**: 1–17. doi:10.1139/cgj-2023-0388.

Taniguchi, I., Yoshida, S., Hiraga, K., Miyamoto, K., Kimura, Y., and Oda, K. 2019. Biodegradation of PET: current status and application aspects. ACS Catalysis, **9**(5): 4089–4105. doi:10.1021/acscatal.8b05171.

van Genuchten, M.Th. 1980. A closed-form equation for predicting the hydraulic conductivity of unsaturated soils. Soil Science Society of America Journal, **44**(5): 892–898. doi:10.2136/sssaj1980.03615995004400050002x.

Vydehi, K.V., and Moghal, A.A.B. 2022. Effect of biopolymeric stabilization on the strength and compressibility characteristics of cohesive soil. Journal of Materials in Civil Engineering, **34**(2). doi:10.1061/(ASCE)MT.1943-5533.0004068.

Wan, Y., Dong, Z., He, X., Liu, R., Cai, Y., Liu, L., et al. 2022. Effect of biochar on permeability of compacted soil and its microscopic mechanism. Canadian Geotechnical Journal, **59**(12): 2184–2195. doi:10.1139/cgj-2021-0586.

Wan, Y., Xue, Q., Liu, L., and Wang, S.Y. 2018. Relationship between the shrinkage crack characteristics and the water content gradient of compacted clay liner in a landfill final cover. Soils and Foundations, **58**(6): 1435–1445. doi:10.1016/j.sandf.2018.08.011.

Wang, L., Ok, Y.S., Tsang, D.C.W., Alessi, D.S., Rinklebe, J., Mašek, O., et al. 2022. Biochar composites: emerging trends, field successes and sustainability implications. Soil Use and Management, **38**(1): 14–38. John Wiley and Sons Inc. doi:10.1111/sum.12731.

Wang, Y., Zhang, A., Ren, W., and Niu, L. 2019. Study on the soil water characteristic curve and its fitting model of Ili loess with high level of soluble salts. Journal of Hydrology, **578**: 124067. doi:10.1016/j.jhydrol.2019.124067.

Wen, T., Wang, P., Shao, L., and Guo, X. 2021. Experimental investigations of soil shrinkage characteristics and their effects on the soil water characteristic curve. Engineering Geology, **284**: 106035. doi:10.1016/j.enggeo.2021.106035.

Yang, F., Xu, Z., Huang, Y., Tsang, D.C.W., Ok, Y.S., Zhao, L., et al. 2021. Stabilization of dissolvable biochar by soil minerals: release reduction and organo-mineral complexes formation. Journal of Hazardous Materials, **412**: 125213. doi:10.1016/j.jhazmat.2021.125213.

Yin, P., and Vanapalli, S.K. 2022. Model for predicting evolution of microstructural void ratio in compacted clayey soils. Canadian Geotechnical Journal, **59**(9): 1602–1621. doi:10.1139/cgj-2021-0057.

Zhang, C.-Y., Han, R., Yu, B., and Wei, Y.-M. 2018. Accounting process-related CO2 emissions from global cement production under Shared Socioeconomic Pathways. Journal of Cleaner Production, **184**: 451–465. doi:10.1016/j.jclepro.2018.02.284.

Zhang, G., Yui, T., Shichi, T., and Takagi, K. 2004. The preparation of clay nanosheets-poly(ethylene terephthalate) hybrid materials. Composite Interfaces, **11**(4): 307–314. doi:10.1163/1568554041738184.

Zhou, X., Lu, X., Wang, Q., Zhu, M., and Li, Z. 2012. Effective catalysis of poly(ethylene terephthalate) (PET) degradation by metallic acetate ionic liquids. Pure and Applied Chemistry, **84**(3): 789–801. doi:10.1351/PAC-CON-11-06-10.

Zong, Y., Chen, D., and Lu, S. 2014. Impact of biochars on swell-shrinkage behavior, mechanical strength, and surface cracking of clayey soil. Journal of Plant Nutrition and Soil Science, **177**(6): 920–926. doi:10.1002/jpln.201300596.